UNIVERSITÄTSBIBLIOTHEK
HANNOVER
TECHNISCHE
INFORMATIONSBIBLIOTHEK

Fossil Hotspot-Ridge Interaction in the Musicians Seamount Province: Geophysical Investigations of Hotspot Volcanism at Volcanic Elongated Ridges

H. Kopp, C. Kopp, W. Weinrebe, E. R. Flueh, J. Phipps Morgan
GEOMAR Research Center for Marine Geosciences, Kiel, Germany

W. J. Morgan
Princeton University, Princeton, USA

[03G142 A]
1999

Abstract

The Musicians Seamount Province is a group of elongate volcanic ridges and single seamounts located north of the Hawaiian Chain. A 327° trending chain of seamounts defines the western part of the seamount province and has been interpreted as the expression of a Cretaceous hotspot beneath the young and northward moving Pacific Plate. To the east, elongated E-W striking ridges dominate the morphology. Similar volcanic elongated ridges (VERs) around the world have been identified from satellite altimetry measurements. Many of these VERs are obviously related to hotspot-ridge interaction, but a number of open questions regarding their structure and origin remain. In 1999, two 400 km long VERs of the Musician seamount group were studied in detail during cruise SO142 of the RV SONNE. Wide-angle seismic data were gathered along four profiles crossing two prominent ridges. In total, 45 OBH (Ocean Bottom Hydrophones) were deployed with a mean spacing of 4 km. We present tomographic images of the volcanic edifices with the aim of identifying the style of volcanism produced by plume-ridge interactions. Our studies of the Musicians VERs indicate that crustal thickening occurs in oceanic layer 2 rather than in layer 3. This extrusive style of volcanism appears to strongly contrast with the formation processes of aseismic ridges, where crustal thickening is mostly accommodated by intrusive underplating of high-velocity lower crust. In addition to the seismic data, high-resolution bathymetry was acquired which yields a detailed image of the morphology of the VERs. From the occurrence of flat-top guyots in the study area and from the unique geomorphologic setting, two independent age constraints for the Pacific crust during the Cretaceous 'quiet' zone are obtained, which allow to present a tectonic reconstruction for the formation of the Musicians VERs that also explains the absence of volcanic edifices north of the Pioneer fracture zone and the re-initiation of volcanism south of the Murray fracture zone. Hotspot-ridge interaction leads to a channeling of melt from the plume to the nearby spreading center over a maximum distance of 400 km. The Musicians VERs were formed by mainly extrusive volcanism on top of this melt channel as the spreading center gradually moved southeastward away from the hotspot, resulting in the observed increasing length of the individual volcanic ridges to the south. The proposed formation model may be applicable to a number of observed volcanic ridges in the Pacific, including the Tuamotu Isles, the eastern portion of the Foundation chain, and the western termination of the Salas y Gomez seamount chain.

UB/TIB Hannover 89
119 621 819

1. Introduction

A great variety of volcanic structures can be observed on the oceanic seafloor. A large fraction of this volcanism has evolved near oceanic spreading centers and different models of hotspot-ridge interaction have been proposed to explain its origin related to this observation. V-shaped ridges or seamount chains, most pronounced at the Reykjanes Ridge south of Iceland or the SE Indian Ridge, are understood to be produced by fixed or moving melt anomalies on a rise axis [Vogt, 1971; Johnson and Vogt, 1973] or the propagation of rift segments [Hey and Vogt, 1977; Sempere et al, 1996]. Broad continuous ridges are often observed where a major plume is centered on a spreading axis. The thickened crust produced by enhanced plume melting leaves trails on the spreading crust like Cocos/Carnegie Ridge [Lonsdale and Klitgord, 1978] or Ninetyeast Ridge [Mahoney et al., 1983]. An additional model for the development of aseismic ridges has been proposed by Morgan [1978], who postulated a sub-lithospheric melt flow from an off-axis hotspot to a spreading center. The additional melt supply increases the volcanic production where the channel reaches the ridge axis and causes the formation of volcanic ridges in the order of 2 km height, which display a distinct azimuth resulting from the sum of the absolute and relative plate motions. The significant new aspect of this idea was that here, the plume and spreading center interact over a distance of up to several hundred kilometers. Isotope geochemical evidence for far-distance interaction between plumes and ridges was subsequently found by a number of studies e.g. Verma and Schilling [1982], Hanan et al [1986], Douglass et al. [1995], [*Yu et al.*, 1997; *Kingsley and Schilling,* 1998]. However, the azimuths of many aseismic ridges in the Atlantic as well as in the Pacific differ significantly from those predicted by the Morgan [1978] model. Aseismic ridges between Clipperton and Galapagos FZ, so-called 'cross-grain ridges' are interpreted to be produced by the filling of tensional cracks in the lithosphere that are caused by the drag of mantle convective rolls [*Winterer and Sandwell*, 1987]. Searle et al. [1995] and Binard et al., [1996] describe morphologically similar ridges west of the Easter Microplate, which they also interpret to be caused by lithospheric tension but in this case, due to thermal, tectonic or volcanic load processes. For the formation of the Pukapuka ridges in the Central Pacific, Sandwell et al. [1995] propose a diffuse extension model which they relate to slab-pull forces affecting the Nazca and Pacific plate boundaries.

In the last decades, several near-axis topographic lineaments and seamount chains within a range of 0-200 km distance to the Mid-Atlantic Ridge (MAR) or East-Pacific Rise (EPR) have been described with orientations that likewise cannot be explained by either absolute or relative plate movement. Small [1995] suggests that a hotspot may be incrementally attracted by the center of an approaching spreading segment producing oblique volcanic trails as observed e.g. at Hollister Ridge, located obliquely between the EPR and the Louisville hotspot track. Other than described by Morgan [1978], in his model the deflected plume channel erupts on the ridge flanks and only in the latest stage on the ridge axis, where the melt is spread along the axis terminating the volcanic trail. From geochemical studies Geli et al. [1998] and Vlastelic et al. [1998] show evidence that excludes a contribution of the Louisville hotspot to Hollister Ridge. They relate the volcanism to intraplate deformation processes.

The ridge trends observed by Schouten et al. [1987] and Clague et al. [2000] near the EPR and MAR again fit perfectly to the trend predicted by Morgan's vector diagrams, although the appearance of the ridges seems to exclude hotspot influence. The axis-parallel motion component of the hotspot is replaced here by a sub-axis asthenosphere flow that equals the motion of the hotspot frame (but not a certain hotspot) with respect to the ridge and the authors interpret the structures to be generated by the migration of asthenosphere-entrained volcanic segments along the ridge. One of the most prominent examples for the off-axis formation of volcanic ridges due to hotspot-ridge interaction is the eastern tip of the Foundation Seamount chain [*O'Connor et al.*, 1998]. Here, the production of individual seamounts produced by the Foundation hotspot switches to elongated ridges as the Pacific-Antarctic Ridge (PAR) approaches the hotspot [*Maia et al.*, 2000]. This behavior is interpreted to reflect the onset of plume-asthenosphere channeling towards the PAR. Most studies on aseismic ridges are based on hydroacoustic and gravimetric measurements. Deeply penetrating seismic investigations revealing deep crustal structures of aseismic ridges have recently been conducted at the Ninetyeast Ridge [*Grevemeyer et al.*, 2001], Cocos Ridge [*Walther*, 2001], Carnegie Ridge [*Flueh et al.*, 2001], Nazca Ridge [*Bialas and Kukowski*, 2000], and Faroe-Iceland Ridge [*Staples et al.*, 1997]. These ridges are formed at spreading centers interacting with a near or on-axis hotspot which results in the typical azimuthal orientation following the projection of the hotspot track and the spreading direction.

The Musicians seamount region (Fig. 1), which is the target of this study, is characterized by a number of roughly W-E trending ridges whose origin is still under discussion. The ridges are slightly oblique to the former relative plate movement and also do not fit the absolute Pacific Plate movement. Epp [1978, 1984] proposed a creation of the ridges by flow of hotspot magma into weak transform faults that parallel the major fracture zones. This interpretation was reinforced in a tectonic reconstruction for the Pacific and Farallon Plate evolution around 90 Ma by Sager and Pringle [1987]. The authors argue that a change in spreading direction might have induced extension along fracture zones, where magma ascended to the surface. The Musicians elongated ridges are situated west of the former Pacific-Farallon spreading center position and do not extend beyond the trail of the Euterpe hotspot to the west (so termed by Flueh et al. (1999) after a muse of musicians in Greek mythology), suggesting that they might be a direct expression of plume-ridge interaction. We propose that the ridges were formed by off-axis volcanism on top of a sub-lithospheric melt flow from the hotspot to the Pacific-Farallon spreading center as this model explains most of the observed features. We use new seismic wide angle and swath bathymetric data to investigate the impact of this kind of volcanism on the crustal structure and morphology and propose a reconstruction model for the Mesozoic Pacific in the Musicians province based on two independent geomorphologic observations.

2. Tectonic setting

The Musicians seamounts are located several hundred kilometers northwest of the Hawaiian chain (Fig. 1). They are separated into a northern and a southern volcanic province by the Murray fracture zone. Seafloor mapping based on satellite altimetry [*Sandwell and Smith,* 1997] reveals several elongated volcanic ridges (VERs), which contain isolated volcanic summits along their crests. The lateral extent of the ridges increases southwards in the northern and southern provinces, respectively (Fig. 1) from less than 100 km to more than 400 km length. Two of the most prominent ridges, the northern Italian Ridge and the southern Bach Ridge (Fig. 1), both trending in a W-E direction nearly parallel to the pronounced fracture zone in their vicinity, are the focus of this study. Their seamounts are found in variable water depths of 2.2 km to 5.1 km (Fig. 2). The Murray Fracture Zone, which crosses the Musicians Province, is approximately 130 km wide (Fig. 3) and displays a ridge-and-trough morphology. As no discernable offset of the Musician seamounts across the fracture zone is observed, several authors [*Freedman and Parsons,* 1986; *Sager and Pringle,* 1987] have suggested that the Musicians were emplaced after fracture activity ceased.

A linear, 327° trending volcanic chain defines the western boundary of the Musicians province, where the elongated volcanic ridges are only recognized to the east and distinctly terminate at the Cretaceous Euterpe hotspot track. Ar-Ar age datings from Pringle [1992] confirm the hotspot hypothesis for this chain and reveal ages between 96 Ma in the north and 82 Ma in the south with a progression rate of 57 km/Ma, which makes it one of the oldest hotspot tracks on the Pacific plate. The Euterpe hotspot track terminates at the Pioneer Fracture Zone (Line 'A' in Fig. 3), which parallels the Mendocino Fracture Zone to the north (Fig. 3). Prior to 96 Ma, the hotspot trail altered the Farallon plate north of the large offset (800-1000 km) Mendocino transform fault before the northwestward moving Pacific Plate moved over the hotspot. Today, all traces on the Farallon plate have vanished since its track has been subducted underneath North America [*Sager and Pringle,* 1987].

The age of the underlying Pacific crust is not clear, as it is formed during the 'quiet' period of the earth magnetic field in the Cretaceous (approx. 118-83 Ma) when the Earth's magnetic field did not reverse its polarity. Extrapolation of the magnetic anomalies by Mueller et al. [1997] yields crustal ages beneath the Musician Seamount Province of approximately 110 Ma with a period of extremely rapid spreading between 120-110 Ma followed by slower spreading with only 1/3 of the rapid opening rate. This would imply that the Musicians were formed on approximately 15 Ma old crust. Freedman and Parsons [1986] propose a much younger age of the seafloor at the time of the seamount emplacement. Their investigations on the crustal elastic thickness yields a lithospheric age of less than 5 Ma at the time the Musicians were formed [*Freedman and Parsons,* 1986].

3. Data acquisition and processing

The HULA field campaign conducted with the German RV SONNE in 1999 [*Flueh et al.,* 1999] investigated two of the most prominent Musicians ridges in detail. To classify their type of volcanism with reference to other marine volcanic ridges and examine the formation of these ridges, the northern Italian Ridge and the southern Bach Ridge have been covered with wide-angle seismic, magnetic (Bill Sager, manuscript in prep., 2002), and hydroacoustic measurements. Geochemical analyses and age dating of several dredge samples along the ridges is still in progress. Here, we present seismic wide-angle data that were collected along three lines across the ridges supplemented by high-resolution swath bathymetric images of the entire length of Italian and Bach Ridge. The seismic lines (Fig.1) are between 180 and 220 km long and on each of them, 12-14 OBH (Ocean Bottom Hydrophones) were placed in the central part of the lines with a mean spacing of 5 km. We used two Bolt air guns with a total volume of 64 l as seismic source. With a shot interval of 60 s and a speed of 4 kn, a shot spacing of about 120 m was achieved. The data were recorded after anti-alias filtering at a sampling rate of 5 ms. In contrast to a well-tuned air gun array, the two large guns produced a rather oszillating signal. However, the seismic signal could be improved significantly by a processing sequence that was adapted to the special data characteristics. We applied a time-gated Wiener deconvolution with a gate length of 2 s. Filtering of wide-angle seismic records has to be done carefully, as the frequency content differs not only with travel time but also laterally with the travel path, whereas attenuation in the water column is neglectable. To account for these difficulties we applied a static water depth correction of the traces prior to an offset and time dependent frequency filter.

High-resolution hydroacoustic seafloor mapping was conducted along the Italian Ridge and the Bach Ridge (Fig. 2) using RV SONNE's onboard Hydrosweep multibeam system [*Grant and Schreiber,* 1990] with a 90° beam angle. Subsequent processing of each sweep was carried out using mbsystem [*Caress and Chayes,* 1996] and gmt [*Wessel and Smith,* 1991]. Sound velocity was determined by CTD measurements [Flueh et al., 1999].

4. Morphology of the Musicians Volcanic Elongated Ridges (VERs)

Global satellite altimetry data [*Sandwell and Smith,* 1997] suggest the Musicians to consist of mostly continuous ridges trending W-E. The new bathymetric data reveal details of the ridge morphology. In Figure 2, the 'predicted bathymetry' [*Sandwell and Smith,* 1997] is overlain by the high-resolution swath mapping data of Italian Ridge and Bach Ridge. The general 90° trend is overlain by oblique en-echelon segments trending about 84°, most obvious at the Italian Ridge in Fig. 2b. The ridges have a mean height of 2000 m and are dominated by prominent volcanoes emerging to a maximum height of 3500 m above the surrounding seafloor with a spacing from 30 km to 80 km. Despite these dominating volcanoes, the structure is significantly different from the Vance, President Jackson and Taney near-ridge seamounts in the northeastern Pacific as described by Clague et al. [2000], which consist exclusively of circular, isolated seamounts on a linear chain. The overall morphology of the Musicians is rather rough. The volcanism is fairly focused on dedicated ridges, similar to those at the Pukapuka ridges in the central Pacific [*Sandwell et al.,* 1995], but there are also several small volcanic cones with diameters between of 3 and 6 km on the plane seafloor nearby (Fig. 2). Diffuse lithospheric extension has been proposed as the origin process for the Pukapuka ridges [*Sandwell et al.,* 1995], however, the investigated ridges are elongate in the direction of present absolute plate motion, which is not the case for the Musician VERs.

The swath data give clear evidence for at least one major flat-top seamount on Italian and on Bach Ridge, respectively. Guyot 1 (Rossini seamount, Fig. 2a) at the western tip of Italian ridge emerges from the surrounding seafloor by 2950 m. Its shape is ESE-expanded and the flat top measures 11 km x 3 km. Guyot 2 is located on the eastern part of Bach Ridge with a height of 2650 m above seafloor level (Fig. 2 c). The circular flat summit, 3 km in diameter, is part of an ENE-elongated ridge segment. Both Guyot summits reach to a water depth of about 2700 m. Nevertheless, they display different relative heights resulting from different depths of the surrounding seafloor, as the southern part of the Musicians is 300 m shallower due to the younger lithosphere south of the Murray FZ and the influence of the nearby Hawaiian swell. The highest volcanoes on the two investigated ridges are labeled with water depths in Figure 2 (a) and (c). They have non-eroded tops and. particularly on Bach Ridge, they exceed the height of the Guyots by some hundred meters.

The relation of the Musicians Ridges to the adjacent fracture zones is enigmatic. Because of plate reorganizations in the Cretaceous, the major North Pacific fracture zones show a complex pattern with multiple changes from single fractures to broad scattered relay zones around the Musicians. Nevertheless, the interpolation of the Pioneer and Murray fracture zones as done from the satellite altimetry dataset in Figure 3 shows that their trends around the northern Musicians region correspond perfectly to each other: A simple shift of the Pioneer FZ trend (line 'A' in Fig. 3) matches the northernmost trace of the Murray FZ (line 'B'). The orientation of the southern Musicians ridges is roughly parallel to the Murray FZ, but from SE to NW, the fractures are getting increasingly oblique and the Musicians ridges do not follow this trend. Instead, their orientation remains constant (about 89°) in the whole area, regardless of the fracture trend. As seen in Figure 3, at the northern Italian Ridge the trend deviation is approximately 8°.

5. Tomographic inversion method

The seismic sections (examples presented in Figs. 4 and 5) show good quality data for the three seismic lines. Most of the stations have clear recordings in the whole shot-receiver offset range, up to a maximum of 140 km (e. g. OBH 35 and 47 in Fig. 5). Only in the central part of line 4, some stations display a lower signal-to-noise ratio attenuating phase coherency beyond 50-70 km offset. The seismic sections are strongly affected by the bathymetry of the ridges causing drastic changes in apparent velocities. However, the upper crustal refraction (Puc), lower crustal refraction (Plc) and mantle refraction (Pn) can be clearly differentiated on almost every station and reveal relatively smooth interval velocity structures across the ridges.

We used the FAST tomography code [*Zelt and Barton,* 1998] for our computations. This method is a first-arrival tomography utilizing the 'regularized inversion' on a uniform velocity grid. The velocity models were defined with a grid size of 2 km in x and 0.5 km in z direction. In total, more than 8000 first-arrival travel time picks per line were used for the inversions. The first arrivals up to ~25 km offset are related to upper crustal refractions (phase Puc in Figs. 4 and 5) and merge with only gradual velocity changes into the lower crustal refractions Plc. Together with the mantle reflection PmP these extend to large offsets of up to 100 km with high amplitudes, which is a distinct phenomenon of this dataset (e. g. OBH 09 and OBH 30 in Fig. 4). Between 40 and 100 km, the lower crustal refractions Plc are 'covered' as second arrivals behind the first-arrival mantle refraction Pn. A standard inversion of these travel times using a first arrival tomography scheme would take primarily the upper crustal and the mantle arrivals into account, but there are two problems with this approach: First of all, particularly with this dataset, nearly 1/3 of the travel time information would not be considered when omitting the second arrival refractions between 40 and 100 km offset (i.e. phase Plc), thus resulting in a poor resolution of the lower crust. Secondly, tomographic inversions of active seismic experiments often fail in reproducing upper mantle structures. The forward calculation technique used in the FAST code is capable of handling large velocity contrasts [*Hole and Zelt,* 1995], but a grid-based inversion generally must seek for a smooth solution to explain the observed travel times and fails in resolving sharp velocity contrasts like the crust-mantle boundary. Furthermore, the requirement of a uniform ray coverage is violated by the special geometry of the Pn phases. To overcome these problems the following approach was employed: In order to keep the starting model as simple as possible, we generated a normal oceanic crust velocity model with laterally constant v(z) dependence below the seafloor, according to the 'minimum 1D-model' of Kissling et al. [1994]. As a pure 1D structure would be rather unrealistic at the volcanic dome, the model is adjusted to the known bathymetry and to a realistic 2D structure at the central volcano as shown for line 2 in Figure 6. The approximate travel time fit of the model was achieved by forward ray tracing [*Zelt and Smith,* 1992], and computation of RMS misfits for different models was used to select the best starting model. The resolution of the computed inversion image could be improved by using a 'layer stripping' inversion method with three iterations. In the first step, only travel time picks with offsets up to 25 km were taken into account, yielding an image of the upper crust. Upper crustal velocities were held fixed in the next iterations. In a second step only offsets greater than 25 km have been inverted, aiming at the recovery of lower crustal velocities. The rays through the lower crust are mostly represented by secondary arrivals behind the mantle refraction (Pn). Therefore, the mantle phases have been omitted in this step. Consequently, also the mantle had to be omitted in the starting model resulting in a crust of infinite thickness as shown in Figure 6. The last step then consisted of an inversion for mantle velocities. Forward raytracing of the mantle phases PmP and Pn was used to define the depth of the Moho, which during a subsequent inversion of the mantle refraction Pn was held fixed to investigate the upper mantle velocities.

6. Resolution tests

Prior to the final inversion of the data, a number of synthetic tests have been conducted in order to determine the best combination of inversion parameters by analyzing the resolution of different anomalies. Although a few kilometers is probably a good estimate for the smallest resolved anomalies, the target of these investigations is to unravel larger structures, particularly those giving insight to the mechanisms that have formed the Musicians ridges. The possible formation scenarios should be reflected in the relation of upper to lower crust: If the ridges were formed by tectonic uplift in a compressional regime, the crustal thickness would be unchanged and the Moho would follow the seafloor trend. A plutonic style of volcanism would thicken the lower crust, while extrusive style leads to a thickening of the upper crust, followed by a flexural downbending of the lithosphere. Additionally there might be underplating of molten material below the crust with velocities between crust and mantle values. A simulation of a plate flexure and velocity anomalies in the lower crust is investigated using synthetic tests. With the resolution tests we test if the inversion method is capable of resolving the upper and lower crustal structure and if the data is sensible to the presence of a plate flexure. A possible plate flexure would not yield a characteristic morphologic signature, as the resulting moat would be filled by volcanoclastic material. However, a tomographic inversion would resolve the lower seismic velocities expected here. The velocity model in Figure 6 b was used to calculate synthetic travel times with a source-receiver geometry and coverage of travel time picks identical to the real experiment (Fig. 7). Using these synthetic data and a smooth input model for an inversion should retrieve the simulated crustal characteristics. Random noise was added to the calculated synthetic travel times using the estimated error of the travel time picks in the real data as standard deviation (between 0.03 s at near offsets and 0.12 s at the far offset traces). The general velocity structure of the test model in Figure 6 b is taken with minor simplifications from line 2, including a plate flexure and a lower crustal velocity anomaly, which should be recognized during the inversion process. The smooth input model for the synthetic resolution test is displayed in Figure 6 a, without the plate flexure and without any lower crustal velocity anomaly. In both models, the lower crustal velocities are extrapolated to 20 km depth and mantle phases are neglected as described earlier. Figure 8 a displays the difference between the input model for the synthetic travel time calculation and the starting model for the inversion, respectively (as shown in Figure 6 a and b). The model difference consists of three velocity anomalies, which are retrieved during the inversion. The plate flexure causes two elongated anomalies of -1.1 km/s, while the lower crustal anomaly is of almost circular shape with an amplitude of -0.3 km/s. The inversion parameters as well as the input model derived from the synthetic inversion tests were also applied to the real data. The difference between the input model and the final model for profile 2 is displayed in Figure 8 b and was gained after a separate inversion of the upper and the lower crust (with 3 iterations for each domain). All anomalies are resolved clearly in position, shape, and amplitude. The upper crustal anomalies have only slightly lower amplitudes and also are terminated where the coverage decreases away from the OBH stations. There are artifacts around profile km 30 and 130, but with only small amplitudes. The ray coverage for the inversion cells of line 2 is shown in panel c of Figure 8, where a maximum coverage of up to 1000 hits per cell is achieved. Thus the geometry used during the field campaign allows to resolve crustal structures beneath the positions of the OBH stations and with some restrictions also in the line periphery.

Subsequent inversion of the mantle refraction (Pn) was conducted while keeping the crustal information unchanged. The resulting velocity update is presented in Figure 9 for line 4. The thick lines in the lower image indicate the deflection of the Moho as confirmed by mantle reflections during the forward modeling procedure and held fixed during the mantle inversion. The resulting velocity perturbations show decreased mantle velocities underneath the central volcano, which corresponds to results gained from forward modeling. Testing with different starting velocities and different Moho depths still yielded the same result. The lower image displays the ray coverage during the mantle inversion, where no deep penetration is to be expected, as the mantle refraction travels close along the crust-mantle boundary.

The calculated travel times obtained from the final inversions are plotted on the seismic sections in the lower panels in Figures 4 and 5 and except for minor fluctuations an overall satisfying fit could be achieved.

7. Crustal and upper mantle structure

The final inversion models for all three lines are presented in Figure 10, where the lowermost image shows a representative ray coverage (P04) achieved during the inversion process. A sediment cover is not recognized along either VER. While the upper and lower crust as well as the upper mantle is clearly resolved along all three profiles, varying internal structures along the lines are revealed. The upper image displays the crustal model for line 2, where a downbending of the upper crust is discernable from the trend of the velocity contours and the Moho. The downflexing results in a moat structure adjacent to the central volcano. It cannot be recognized in the morphology, because it is filled with volcanic debris as inferred from the low seismic velocities of less than 3.5 kms^{-1} here. A similar flexural structure is also recognized along profile 4 (Fig. 10 c). This downflexing of the oceanic crust results from a top-loading of the volcanic edifice. The thickened upper crust along these lines implies a ridge evolution dominated by extrusive volcanism above the pre-existing oceanic crust. Velocities increase within the upper portion of the crust from 4.4 kms^{-1} to 6.5 kms^{-1} corresponding to a velocity gradient of approximately 0.9 s^{-1}. The third line (Fig. 10 b) shows a more complex structure as may be expected from the presence of numerous smaller volcanoes around the central volcano, which is not as large and prominent as along the other two lines. No clear flexural bending or moat structure in the upper crust is resolved. It is clearly evident though that the upper crust, which displays equivalent seismic velocities, is characterized by an increased thickness away from the central volcano (Fig. 10 b), which is not the case along the other two lines. The volcanic edifices show increasing velocities with depth (up to 5.7 kms^{-1} for the large central volcanoes on profiles 2 and 3 and up to 6.2 kms^{-1} on profile 4, respectively), as is evident from the upward deflection of the upper crust velocity contours, which mimic the seafloor. The lower crust is characterized by a reduced velocity gradient of 0.13 s^{-1}, with velocities increasing 7.1 kms^{-1}. Along profile 3, the lower crust displays some thickening, as along the other two lines, however, here the zone of thickening is broader than on profiles 2 and 4, where a deflection of the Moho is mainly restricted to the area underneath the central volcano (Fig. 10 a and c). Based on the inversion models an extrusive dominated type of volcanism is inferred for the Musicians, though secondary intrusive processes may not be ruled out. Even though reduced mantle velocities are revealed in a small area underneath the ridge centers (Figs. 9 and 10), underplating is insignificant here, as the seismic data do not show any supplementary reflections near the Moho reflection that may be related to a layer of material underplated beneath the crust. The Moho reflections identified during the forward modeling process (bold lines in Fig. 9) are restricted to the flanks of the thickened portion of the crust and cannot be identified in the central part where lowered velocities have been inferred. Reflection phases caused by underplating are to be expected here and have been found e.g. at Ninetyeast Ridge, Gran Canaria, and Hawaii [*Grevemeyer et al.*, 2001; *Ye et al.*, 1999; *Watts and ten Brink*, 1989]. Figure 11 shows a global compilation of different hotspot related volcanic edifices with an identical scaling. All of these were located directly above a hotspot at the time of their formation and all of these show possible signs of underplating, though different models have been proposed for Hawaii and Canary. For comparison, the Musicians, which are of much smaller size, are displayed at the bottom. Most of the larger volcanic reliefs show indications for intrusive volcanism, whereas extrusive processes seem to be influential in the evolution of the Musicians. The different structure of the Musicians VERs is related to a different formation process, where the volcanoes where not formed on top of a hotspot, but rather in between an off-axis plume and the spreading center.

8. Discussion

The inferred extrusive-type volcanism dominant during the formation of the Musicians seamounts is also supported by the rough morphology of the ridges. The rugged topography implies that the ridges were created by a number of consecutive eruptions with a low effusion rate over a longer period of time. The narrow width of the ridges (approximately 15 km) indicates an off-axis magma source, which is confined in a narrow constructional lineament [*Small*, 1995]. In particular the number of small volcanic cones between the ridges has in earlier papers been seen as an indication that the Musicians were built by magma that erupted preferably through pre-existing fractures in the vicinity and parallel to the Murray FZ [*Lowrie et al.*, 1986; *Sager and Pringle*, 1987; *Pringle*, 1992]. This, however, is contradicted by two observations: the formation of the VERs is terminated at the Murray fracture zone and not increased as would be expected. Within the 130 km wide Murray FZ, several isolated volcanoes have erupted, but do not show an obvious connection to the major faults scarps. The formation of en-echelon ridge segments as observed along e.g. the Italian Ridge (Fig. 2) has been interpreted for other ridges to be caused by deformation processes resulting in tensional cracks [*Winterer and Sandwell,* 1987; *Geli et al.,* 1998; *Vlastelic et al.,* 1998]. However, in the Musicians province the filling of tensional cracks should form en-echelon ridges in the major fracture zones, which are not recognized here. A possible process to create the observed en-echelon segments in the study area may be associated to cracks propagating away from volcanic centers in a regional stress field with tension vectors oblique to the spreading direction [*Kopp and Phipps Morgan,* 2000].

Secondly, from satellite altimetry data it is obvious that the Pioneer FZ and the Murray FZ show an almost perfect parallelity over the northern Musicians province (line 'A' and 'B' in Figure 3). Smaller fracture zones in the stress field between the large prominent fractures should follow this trend, and so should the Musicians VERs if they erupted along smaller fractures as proposed by e. g. Epp (1984) and Sager and Pringle (1987). However, as seen in Figure 3, the Musicians deviate by about 8° from the general fracture zone trend between the Murray and Pioneer FZ. In the south, the emplacement of the ridges along pre-existing fractures is also unlikely, even though the deviation of the Musicians trend from the overall direction of the fracture zones here is not as significant as in the north. While the fracture zone trend changes from south of the Murray FZ to north of it, as indicated by the extrapolated trend in Figure 3, this is not the case for the trend of the Musicians VERs, which implies that a conjunction between the Musicians emplacement and the existence of larger or smaller fracture zones in the area is not given. However, the alignment of all Musicians ridges suggests a common evolution. A possible explanation would be their emplacements above a sublithospheric melt flow directed from the Euterpe hotspot track to the Pacific-Farallon spreading center. As a sublithospheric melt flow would be driven by buoyancy and thus follow the strongest gradient of lithospheric thickness, it would always show a perpendicular orientation to the spreading center. This is supported by the observation that the Musicians VERs are pointing towards a N-S oriented spreading center to the east of the Musicians province (Fig. 3), which is coincident with the last observed magnetic anomaly after the Cretaceous 'quiet' zone (M34 corresponding to 84 Ma in Fig. 3) and is oriented in a N-S direction. This observation does not contradict the fact that the Musicians are not parallel to the major fracture zones, as these will not evolve perpendicular to the spreading center in a phase of oblique spreading. Oblique spreading is inferred from changes in spreading direction which are manifested in the splitting of the fracture zones into extensional relay zones of an en-echelon staircase pattern observed for example along Mendocino FZ between 140°W and 165°W [*Flueh et al.,* 1999].

The magmatic feeding of spreading centers by neighboring mantle plumes over hundreds of kilometers has been suggested by a number of authors [*Vogt,* 1971; *Morgan,* 1978; *Epp,* 1984; *Schilling et al.,* 1985]. From the existence of at least two guyots in the study area (Fig. 2), constraints on the distance of the Pacific Farallon spreading center to the Musicians ridges may be drawn. The flat top Rossini Seamount on the Italian Ridge lies in a water depth of 2.7 km (Fig. 2). From the standard seafloor subsidence assuming 2500 m water depth at the spreading center (Parsons and Sclater, 1977), it is inferred that Rossini Seamount erupted on 1.7 Ma old seafloor. Guyot 2 on Bach Ridge erupted on 0.2 Ma old oceanic lithosphere. Clague et al. [2000] propose that flat top seamounts may also form from collapsing calderas, which are subsequently filled and subdued. However, the Vance, President Jackson or Taney seamounts shown by Clague display a strikingly different morphology compared to the Musicians, with an organized structure consisting of single volcanoes with ring-formed calderas lining up to an entire seamount chain. In contrast, the Musicians guyots have a much more irregular shape and all volcanoes are connected by diffuse ridge volcanism and do not form isolated structures. We believe that the Musicians flat tops were built by erosional processes in shallow water depths near the spreading axis.

The digital magnetic isochrone map of Mueller et al., [1997] suggests a seafloor age of 107 Ma underneath Rossini Seamount near the western termination of Italian Ridge. An evolution of Rossini close to the spreading axis would thus imply that Rossini Seamount must be older than the oldest dredged samples from the Musicians province (maximum 96 Ma). As this is unlikely, we propose an alternative reconstruction of the seafloor underneath the Musicians formed during the Cretaceous 'quiet' zone, which will explain the near-spreading axis location of the guyots at the time of their formation. The geometry of the Musicians offers a second, independent strong age constraint on the tectonic history of the Western Pacific: the reconstruction is based on the morphological geometry in the Musicians province, where the Euterpe hotspot trail ends abruptly in the north. The absence of a hotspot track north of the Mendocino FZ has been explained by the large offset across the fracture zone and the subduction of the Farallon plate [*Sager and Pringle,* 1987]. The oldest Musicians seamount is located just south of the Pioneer FZ with an Ar-Ar determined age of approximately 96 Ma implying that this is the time at which the hotspot crossed the Pioneer FZ. Prior to this time, Euterpe produced seamounts on the Farallon plate. The Pioneer FZ however displays a much shorter offset of ~200 km compared to Mendocino FZ. This is also evident from the surface traces of the fracture zones, where plate reorganizations result in large relay zones and a splitting of the fault from a single trace into a number of oblique sub-parallel tracks along Mendocino FZ, while 'simple' kinks compensate the changes in plate motion along the short-offset Pioneer FZ [*Flueh et al.,* 1999]. As prior to 96 Ma the Pacific-Farallon spreading center north of the Pioneer FZ must have been located westwards of the hotspot track, while being placed eastward of the hotspot trail on the Pacific plate south of the Pioneer FZ, the hotspot must have crossed the Pioneer FZ in a small 'window' determined by the ~200 km offset. Only this geographic setting explains the absence of the hotspot track north of the Pioneer FZ and its simultaneous presence today on the Pacific plate. This observation puts a geographic constraint on the location of the spreading center with regards to the hotspot track at 96 Ma. From this follows that the spreading center was located at a distance between 0 and 200 km east of the hotspot track. From the dating of magnetic anomalies [*Atwater and Severinghaus,* 1989] the first position of the spreading center after the Cretaceous 'quiet' zone is known (M34 at 84 Ma). Interpolation then yields the approximate former positions of the spreading center in the Musicians province at the time of the VER emplacement (Fig. 12).

The observed guyots offer a second independent constraint on this reconstruction. Rossini seamount, which was inferred to have been emplaced on 1.7 Ma crust, fits adequately to the new reconstruction, where it would be placed on approximately 2 Ma old crust. Judging from the height of the second guyot, which is located toward the eastern end of Bach Ridge, it must have been created on 0.2 Ma old crust. The reconstruction would place it on ca. 0.5 Ma old crust. Thus for both flat tops a mean error of less than 0.5 Ma is inferred for the tectonic reconstruction.

Sager and Pringle [1987] proposed a tectonic model for the formation of the Musicians, which involves a long section of Farallon plate that protruded into the Pacific plate. A change in spreading direction at approximately 90 Ma, as evidenced by the extensional relay zones along the neighboring fracture zones, induced the eruption of hotspot magma along fractures and cracks caused by the resulting tensional deformation. The corresponding change in the fracture zone trend to a staircase pattern has an approximate distance of 290 km to Rossini seamount. Assuming a spreading rate between 4.4 cm/a [*Mueller et al.,* 1997] and 7.4 cm/a (this study) this implies that Rossini must have been built on 6.6 Ma or 3.7 Ma old crust, respectively, which would have subsided too far for the flat top volcanoes to form and stands in contradiction to the 1.7 Ma computed from the depth of the eroded top. Another important aspect that cannot be explained by the model proposed by Sager and Pringle is the observation that the ridges terminate at the hotspot track. This geometry is best explained by a model based on hotspot-ridge interaction.

Based on the newly acquired geophysical data presented here a possible evolution scenario for the Musicians VERs has been developed and is displayed in Figure 13. The Euterpe hotspot was close enough to the Pacific Farallon spreading center that melt could flow beneath the lithosphere to the spreading axis and feed it. The Euterpe mantle plume leaves a regular hotspot track on the Pacific plate. It marks the exact western termination of the VERs, which develop on top of a melt flow channel from the hotspot to the spreading center. Hotspot-ridge interaction has been shown to cause the development of aseismic ridges like Ninetyeast Ridge or Cocos Ridge by the production of thickened crust where hotspot melt contributes to the production of crust at the spreading center. In principle, this mechanism may also apply for off-axis hotspots erecting an aseismic ridge as described by Morgan (1978) with a distinct azimuth which equals the sum of the absolute plate motion over the hotspot and the relative plate motion along the spreading direction. However, in this scenario an aseismic ridge would have an orientation as indicated by the stippled line in Figure 13, which significantly differs from the trend of the observed VERs. The location and geometry of the Musicians ridges rather imply that they were built all the way on top of the melt channel, the shortest path between hotspot and spreading center and perpendicular to the spreading axis, as discussed above. The eastern termination of the VERs is then given by the former position of the spreading axis at the time of the volcanic ridge emplacement (Fig. 12). Between 96 Ma and 84 Ma, the distance between hotspot and spreading center was progressively increased by the southeastward movement of the spreading center, resulting in an increasing W-E extension of the VERs until the distance between the hotspot and the spreading center grew too large for a magma flow to develop south of Italian Ridge at 91 Ma. An evolution of the Musicians VERs by interaction of the Euterpe Hotspot and the Pacific-Farallon spreading center also explains the observation that ridge formation is re-initiated south of the Murray FZ: due to the offset across the Murray FZ, the spreading center was at 81 Ma again close enough to the hotspot for VERs to form between them (Fig. 12). As expected here, the VERs again show increasing lengths to the south.

Not only in the case of the Musicians has it been observed that aseismic ridges in the vicinity of spreading centers resulting from hotspot-ridge interaction often do not follow the azimuth predicted by Morgan [1978], though plume-ridge interaction seems to play a major role in their evolution [*Morgan,* 1978; *Schilling,* 1985; *Small,* 1995]. Numerical models by Ito [1997] infer a maximum possible distance of plume-ridge interaction, which scales with plume source volume flux and ridge spreading rate, implying that there is an upper limit to the hotspot-spreading center separation as is proposed for the Musicians. The plume affects the ridge in a number of ways: the geochemical signature shows signs of plume enrichment (as reported for e. g. lead isotope ratios [*Kingsley and Schilling,* 1998]) and could additionally affect the topography and crustal thickness in the vicinity of the ridge [*Maia et al.,* 2000]. This also depends on the effectiveness of the melt channeling as there seems to be a difference in the amounts of plume material reaching the ridge axis for different ridge-hotspot systems [*Maia et al.,* 2000]. The area over which the ridge is affected by the plume is 125-200% as broad as the maximum plume ridge separation, so that the excess plume melt is distributed over a large segment of the ridge and possibly does not cause changes in topography or crustal thickness [*Ito et al.,* 1997]. We propose that this scenario applies to the Musicians. The VERs are terminated to the east at the assumed former position of the spreading axis where the excess melt is distributed along-axis. This explains why no 'Morgan-type' aseismic ridges following the predicted azimuth (stippled line in Fig. 13) are observed here.

For the Western Easter Salas y Gomez seamount chain focused flow along an approximately 70 km wide channel towards the EPR has been proposed by Kingsley et al. (1998). Their Pb isotope investigations are not compatible with a passive radial melt mixing here. The observation of a neovolcanic gap close to the EPR may be associated with counteractive flow away from the EPR or by a capturing and focusing of the plume material by the upwelling system of the ridge [*Kingsley and Schilling,* 1998]. As the former position of the Pacific Farallon plate with regards to the Musicians VERs may be inferred from the formation depths of the guyots in the study area, a similar volcanic gap in the Musicians province is unlikely, implying that the maximum length of the VERs corresponds to the maximum hotspot-ridge interaction distance as discussed by Ito et al., (1997).

9. Conclusions

The Musicians volcanic elongated ridges were formed by plume-hotspot interaction on top of sublithospheric melt channels between the Euterpe hotspot track and the Pacific-Farallon spreading center. This model is supported by the geometry, ages, and bathymetry of the investigated volcanoes. The Musicians volcanoes form coherent volcanic ridges, which show a mostly extrusive style of volcanism as inferred from the tomographic investigations of the newly acquired seismic data presented here. Crustal thickening is recognized in oceanic layer 2 rather than in layer 3. Although reduced seismic velocities in the upper mantle were recorded, these could not be associated with underplating here. The extrusive mode of formation stands in contrast to the seismic structure of many aseismic ridges, where crustal thickening is mostly accommodated by intrusive underplating of high-velocity lower crust. The progressively increasing lengths of the Musicians VERs from north to south are a distinct feature of this volcanic province. From this morphological geometry a maximum hotspot spreading center separation of approx. 400 km, over which sublithospheric plume-ridge interaction occurred, is observed. Another important aspect of this study is the recognition of two independent age constraints for the Pacific crust during the Cretaceous 'quiet' zone. From the existence of guyots in the Musicians province the former location of the Farallon-Pacific spreading center may be inferred. Its position at 96 Ma just south of the Pioneer FZ may additionally be derived from the unique geometrical setting here, which yields a 'window' of maximum 200 km width for Euterpe hotspot to pass from underneath Farallon plate, where its track east of the spreading center was ultimately destroyed, to the Pacific plate, where it was located west of the ridge. Assuming that the Musicians VERs developed in conjunction with Euterpe hotspot, as is highly likely due to the western termination of the ridges at the hotspot track, a tectonic reconstruction of this area of the Pacific during the Cretaceous 'quiet' zone has been developed which differs by up to 10 Ma from the isochrone age map by Müller et al.

The proposed formation scenario may be applicable to a number of aseismic ridges observed near spreading centers. Along the Eastern termination of the Foundation Chain, which approaches the PAR, a change in fabric from the isolated seamounts caused by the passing of the Pacific plate over the Foundation plume to a broad region of en-echelon ridges similar to the Musicians VERs is observed [*O'Connor et al.*, 1998]. The Tuamotu Isles east of Tahiti form the subaerial trace of en echelon ridges, which may represent fossil VERs in the Central Pacific [*Searle et al.*, 1995]. Another example for a volcanic ridge formed on top of a sublithospheric plume flux is the western Easter-Salas y Gomez seamount chain as proposed by Kingsley [1998], where none of the seamounts are associated with any of the apparent fracture zones, as is the case for the Musicians VERs.

Acknowledgments. We thank all participants of the HULA cruise and especially Capt. Papenhagen and his crew for their professional work at sea. The HULA project is supported by the German Federal Ministry for Science and Technology (BMBF).

References

Atwater, T., and J. Severinghaus, Tectonic maps of the northeast Pacific, in: Winterer, E. L., Hussong, D. M., and Decker. R. W. (eds) *The Eastern Pacific Ocean and Hawaii*, The Geology of North America, Vol. N., Geological Society of America, 15-20, 1989.

Caress. D. W., and D. N. Chayes. Improved processing of Hydrosweep DS multibeam data on the R/V Maurice Ewing, *Marine Geophysical Research*, *18*, 631-650. 1996.

Clague, D. A., J. R. Reynolds, and A. S. Davis, Near-ridge seamount chains in the northeastern Pacific Ocean, *Journal of Geophysical Research, 105*, 16541-16561, 2000.

Bialas, J., N. Kukowski (edt) and Shipboard Science Party, GEOPECO (SONNE Cruise SO-146): Geophysical Experiments at teh Peruvian continental margin, *Cruise Report, Geomar, Kiel*, 2000.

Binard, N., P. Stoffers, R. Hekinian, R. C. Searle, Intraplate en echelon volcanic ridges in the South Pacific west of the Easter microplate, *Tectonophysics, 263,* 23-37, 1996.

Epp, D., Possible perturbations to hotspot traces and implications for the origin and structure of the Line Islands, *Journal of Geophysical Research, 89,* 11273-11286, 1984.

Flueh, E.R., J. O'Connor, J. Phipps Morgan, J. Wagner (edts) and Shipboard Science Party, HULA (SONNE Cruise SO-142): Interdisciplinary investigations on the timing of the Hawaii-Emperor Bend and the origin of lithospheric anomalies along the Musician seamount chain, *Cruise Report, Geomar, Kiel*, 1999.

Flueh, E.R., J. Bialas, P. Charvis (edt) and Shipboard Science Party, SALIERI (SONNE Cruise SO-159): South American Lithospheric Transects Across Volcanic Ridges, *Cruise Report, Geomar, Kiel*, 2001.

Freedman, A. P. and B. Parsons, Seasat-Derived Gravity over the Musicians Seamounts, *JGR, 91,* 8325-8340, 1986.

Geli, L., D. Aslanian, J.-L. Olivet, I. Vlastelic, L. Dosso, H. Guillou, and H. Bougault, Location of Louisville hostpot and origin of Hollister Ridge: geophysical constraints, *Earth and Planetary Science Letters, 164,* 31-40, 1998.

Grant, J. A. and R. Schreiber, Modern swath sounding and subbottom profiling technology for research applications: The Atlas Hydrosweep and Parasound systems, *Int. Marine Geophysical Research, 12*, 9-19, 1990.

Grevemeyer, I., E. R. Flueh, C. Reichert, J. Bialas, D. Klaeschen, and C. Kopp, Crustal architecture and deep structure of the Ninetyeast Ridge hotspot trail from active-source ocean bottom seismology, *Geophys. J. Int., 144*, 1-22, 2001.

Hole, J. A., and B. C. Zelt, 3-D finite-difference reflection traveltimes, *Geophys. J. Int., 121*, 427-434, 1995.

Ito, G., J. Lin, and C. W. Gable, Interaction of mantle plumes and migrating mid-ocean ridges: Implications for the Galapagos plume-ridge system, *J. Geophys. Res., 102*, 15403-15417, 1997.

Kingsley, R. H., and J.-G. Schilling, Plume-ridge interaction in the Easter-Salas y Gomez seamount chain-Easter Microplate system: Pb isotope evidence, *JGR, 103*, 24159-24177, 1998.

Kissling, E., W. L. Ellsworth, D. Eberhart-Phillips, and U. Kradolfer, Initial reference models in local earthquake tomography, *JGR, 99,* 19635-19646, 1994.

Kopp, C. and J. Phipps Morgan, Is the en-echelon formation of volcanic elongated ridges due to interacting 'dike-like' magma propagation away from discrete volcanic centers?, *EOS Trans. AGU, 81 (48),* Fall Meet. Suppl., 2000.

Lowrie, A., C. Smoot, and R. Batiza, Are oceanic fracture zones locked and strong or weak?: New evidence for volcanic activity and weakness, *Geology, 14,* 242-245, 1986.

Maia, M., Ackermand, D., Dehghani, G. A., Gente, P., Hekinian, R., Naar, D., O'Connor, J., Perrot, K., Phipps Morgan, J., Ramillien, G., Revillon, S., Sabetian, A., Sandwell, D., and Stoffers, P., The Pacific-Antarctic Ridge-Foundation hotspot interaction: a case study of a ridge approaching a hotspot, *Marine Geology, 167,* 61-84, 2000.

Morgan, W.J., Rodriguez, Darwin, Amsterdam ,..., A Second type of Hotspot Island, *JGR, 83* 5355-5360, 1978.

Mueller, D., W. R. Roest, J. Y. Royer, L. M. Gahagan, and J. G. Sclater, Digital Isochrons of the world's Ocean Floor *JGR, 102* 3211-3214, 1997.

O'Connor, J. M., P. Stoffers, and J. R. Wijbrans, Migration rate of volcanism along the Foundation Chain, SE Pacific, *EPSL, 164,* 41-59, 1998.

Pringle, M. S., Geochronology and Petrology of the Musicians Seamounts, and the search for hot spot volcanism in the Cretaceous Pacific, *PhD Thesis, Universitz of Hawaii,* 1992.

Pringle, M. S., Age progressive volcanism in the Musicians seamounts: A test of the hot spot hypothesis for the late Cretaceous Pacific,in: The Mesozoic Pacific: Geology, Tectonics, and Volcanism, *Geophysical Monograph 77,* 187-215, 1993.

Sager, W. W. and M. S. Pringle, Paleomagnetic constraints on the origin and evolution of the Musicians and South Hawaiian Seamounts, Central Pacific Ocean,in: Seamounts, Islands, and Atolls, *Geophysical Monograph 43,* 133-162, 1987.

Sandwell, D. T., E. L. Winterer, J. Mammerickx, R. A. Duncan, M. A. Lynch, D. A. Levitt, and C. A. Johnson, Evidence for diffuse extension of the Pacific Plate from Puka-puka ridges and Cross-grain gravity lineations, *JGR, 100* 15087-15099, 1995.

Sandwell, D., and W. H. F. Smith, Global marine gravity from Geosat and ERS-1 Satellite Altimetry, *JGR, 102,* 10039-10054, 1997.

Schilling, J.-G., G. Thompson, R. Kingsley, and S. Humphris, Hotspot-migrating ridge interaction in the South Atlantic, *Nature, 313* 187-191, 1985.

Schilling, J.-G., Upper mantle heterogeneities and dynamics, *Nature, 314* 62-67, 1985.

Schouten, H., H. J. B. Dick, and K. D. Klitgord, Migration of mid-ocean-ridge volcanic segments, *Nature, 326* 835-839, 1987.

Searle, R. C., J. Francheteau, and B. Cornaglia, New observations on mid-plate volcanism and the tectonic history of the Pacific plate, Tahiti to Easter microplate, *EPSL, 131* 395-421, 1995.

Small, C. Observations of ridge-hotspot interactions in the Southern Ocean, *JGR, 100* 17931-17946, 1995.

Staples, R., R. White, B. Brandsdottir, W. Menke, P. Maguire, and J. McBride, Faroes-Iceland Experiment 1: The crustal structure of Northeastern Iceland, *JGR, 102* 7849-7866, 1997.

Vlastelic, I., L. Dosso, H. Guillou, H. Bougault, L. Geli, J. Etoubleau, and J. L. Joron, Geochemistry of the Hollister Ridge: relation with the Louisville hotspot and the Pacific-Antarctic Ridge, *EPSL, 160,* 777-793, 1998.

Vogt, P. R., Astenosphere motion recorded by the ocean floor south of Iceland, *EPSL, 13,* 153-160, 1971.

Walther, C. H. E., The crustal structure of the Cocos Ridge off costa Rica, *JGR,* , submitted, 2001.

Watts,A. B., and U. S. ten Brink, Crustal Structure, Flexure, and Subsidence History of the Hawaiian Islands, *J. Geophys. Res., 94,* 10473-10500, 1989.

Wessel, P., and W. H. F. Smith, Free software helps map and display data, *EOS Trans. AGU, 72, 441* 445-446, 1991.

Winterer, E. L., and D. T. Sandwell, Evidence from en-echelon Cross-grain ridges for tensional cracks in the Pacific Plate, *Nature, 329,* 534-535, 1987.

Ye, S., J. P. Canales, R. Rihm, J. J. Danobeitia, and J. Gallart, A crustal transect through the northern and northeastern part of the volcanic edifice of Gran Canaria, Canary Islands, *Journal of Geodynamics, 28,* 3-26, 1999.

Yu, D., D. Fontignie, J.-G. Schilling, Mantle plume-ridge interactions in the Cental North Atlantic: A Nd isotope studz of Mid-Atlantic Ridge basalts from 30N to 50N, *EPSL, 146,* 259-272, 1997.

Zelt, C. A., and P. J. Barton, Three-dimensional seismic refraction tomography: A comparison of two methods applied to data from the Faeroe Basin, *Journal of Geophysical Research, 103,* 7187-7210, 1998.

Zelt, C. A., and R. B. Smith, Seismic traveltime inversion for 2-D crustal velocity structure, *Geophys. J. Int., 108,* 16-34, 1992.

E. R. Flueh, C. Kopp, H. Kopp, J. Phipps Morgan, W. Weinrebe GEOMAR Research Center for Marine Geosciences, Wischhofstr. 1-3, 24148 Kiel, Germany. (e-mail: eflueh@geomar.de, ckopp@geomar.de, hkopp@geomar.de, jmorgan@geomar.de, wweinrebe@geomar.de)

W. J. Morgan, Princeton University, Princeton, NJ 08544-1003, USA. (e-mail: wjmorgan@geo.princeton.edu)

Received April 1, 2002; revised xxx xx, 2002; accepted ? ?, ?.

This preprint was prepared with AGU's LaTeX macros v5.01. File Hula formatted March 22, 2002.

Figure 1. Location map of the Musician seamounts north of the Hawaiian chain. The 327° trending Cretaceous Euterpe hotspot track marks the western boundary of the volcanic province. No evidence for volcanism is found north of the Pioneer fracture zone. The Musician volcanic elongated ridges (VERs) trend in an E-W direction. The Murray fracture zone splits the study area in a northern volcanic regime and a southern volcanic area. The increasing length of the ridges from north to south in the two volcanic areas is a unique feature of this province and together with the abrupt termination of the ridges at the hotspot track has been explained by hotspot-ridge interaction which forms a melt channel in between Euterpe and the fossil Pacific-Farallon spreading center to the east. Geophysical investigations were conducted along the northern Italian Ridge and the southern Bach ridge. Wide-angle seismic data were acquired along four profiles and are complemented by high-resolution bathymetric data.

Figure 2. High resolution bathymetric images of the two most prominent ridges in the Musician volcanic province. The swath data is underlain by predicted bathymetry from satellite altimetry data (Sandwell and Smith, 1997) (b and d). The coherent ridges are up to 400 km long and are characterized by distinct volcanic cones and en echelon segments. In the side view displayed in a and c at least one guyot along Italian Ridge and Bach Ridge, respectively, is recognized. From the height of the erosional flat-tops the distance of the guyots to the Pacific-Farallon spreading ridge at the time of their formation may be inferred and yields an independent constraint for the age of the Pacific crust.

Figure 3. Interpolated fracture zone trends between Pioneer and Murray Fracture zones (A and B) deviate by about 8° from the trend of the Musician VERs. Thus their origin cannot be associated with the apparent fracture zones. Thick black lines indicate magnetic anomalies before the Cretaceous quiet zone. M33 and M34 correspond to approximately 75 Ma and 84 Ma, respectively.

Figure 4. Seismic wide-angle sections for OBH09 of Line 02 (upper images) and OBH30 of Line 03 (bottom images). The lower displays illustrate the calculated traveltimes on top of the seismic data which are shown in the upper displays. Clear phases from the lower crust (Plc) and mantle (Pn) to offsets reaching 100 km are observed on a number of stations. The pronounced morphology of the volcanic province is also recognized in the seismic arrivals. The tomographic inversion applied to the data employs primary as well as secondary arrivals to include a maximum of traveltime information. Successive inversion of different offset ranges recovered the crustal velocities using a top-to-bottom approach.

Figure 5. Seismic wide-angle sections for OBH35 and OBH47 of Line 04 across Bach Ridge. Please refer to Figure 4 for display information. 12 to 14 instruments were deployed on each profile discussed in the text.

Figure 6. The upper image displays the input starting model for the inversion using crustal arrivals. Morphology information from the profiles is included in the starting model, which assumes a standard oceanic crust. As mantle phases were omitted during this stage of the inversion, the model displays a crust of infinite thickness. The calculated inversion of the crustal arrivals is displayed in the lower image and is used as the input model for the synthetic data calculation. The inversion model displays a flexural downbending of the crust centered beneath the volcanic edifice and a velocity anomaly in the lower crust.

Figure 7. Synthetic travel time picks were generated using the source-receiver geometry and bathymetry of the experiment. Coverage of the travel time picks is identical to the real experiment. The synthetic data are used for resolution tests to verify if the crustal characteristics of the test model displayed in Fig. 6b may be retrieved with the experiment layout. The smooth input model for the synthetic resolution test is displayed in Fig. 6a. Both models are used to image the crust and thus neglect any mantle phases.

Figure 8. a) displays the difference between the input models for the synthetic travel time calculation and for the inversion, respectively, as displayed in Fig. 6 a and b. The model difference is characterized by three velocity anomalies, which must be retrieved by the inversion process. The plate flexure causes two elongated anomalies of -1.1 km/s. A lower crustal anomaly of almost circular shape has an amplitude of -0.3 km/s. The difference between the input model and the final model applied to the real data of line 02 is displayed in b), where all anomalies are clearly resolved in position, shape, and amplitude. The lowermost image displays the ray coverage achieved for the inversion cells of profile 02 with a maximum coverage of 1000 hits per cell.

Figure 9. The mantle refraction Pn was inverted while keeping the crustal information unchanged. The velocity update is displayed in the upper image. The position of the Moho (indicated by the thick black lines in b) is inferred from forward modeling of the mantle reflections and is kept fix during the mantle inversion. Decreased mantle velocities are observed underneath the central volcano and were always retrieved for different starting velocities and Moho depths. Panel b) displays the ray coverage during the mantle inversion.

Figure 10. Final inversion models for all three profiles and corresponding residuals. Line 02 and 04 display a flexural downbending of the crust. The thickened upper crust along all profiles is indicative of extrusive volcanism above the pre-existing oceanic crust. The lower crust displays a decreased velocity gradient compared to the upper portion and a deflection of the Moho underneath the central volcano. Clear evidence for underplating is not observed on any of the lines. Residuals were computed using crustal phases. The lower panel shows the ray coverage along profile 04.

Figure 11. Global compilation of different hotspot related volcanic structures. All examples are scaled identically. Separation between upper and lower crust along all models is based only on velocities. Intrusive volcanism and underplating are characteristic for these volcanic provinces, which were located above a hotspot at the time of their formation. The Musicans are displayed at the bottom. They show much smaller dimensions and a dominated by extrusive volcanism. Their formation is linked to hotspot-ridge interaction, as they evolved between the Euterpe hotspot and the Pacific-Farallon spreading center.

Figure 12. Proposed tectonic reconstruction based on geomorphological observations in the study area north of the Hawaiian seamount chain. The northwestward trending line is the track of the Cretaceous Euterpe hotspot with its age progression indicated in Ma. The hotspot crossed the Pioneer fracture zone at approximately 97 Ma. Its track north of the FZ has been destroyed with the subduction of the Farallon plate. The former position of the Pacific-Farallon spreading center is indicated by the stippled lines and has been inferred from the crossing time of Euterpe over Pioneer FZ and from magnetic anomalies before the Cretaceous 'quiet zone'. The position of guyots with respect to the spreading center yields a second, independent age constraint. The spreading center progressively moved away from Euterpe hotspot from north to south, until being shifted closer to the hotspot again by the offset across the Murray FZ. The Musicians VERs were formed between the hotspot and the spreading center, which explains their progressively increasing lengths and their westward termination at the hotspot track. When the distance between Euterpe and the spreading center grew too large at 93 Ma, formation of the VERs stopped, but was re-initiated south of the Murray FZ.

Figure 13. Formation of the Musicians VERs between the Euterpe hotspot and the Pacific-Farallon spreading center. When the hotspot was close enough to the ridge that melt could flow beneath the lithosphere to the spreading axis and feed it, volcanic elongated ridges developed on top of the melt channel. Their orientation is perpendicular to the spreading center and thus differs from the azimuth of an aseismic ridge originating at the spreading center. The latter shows an orientation as indicated by the stippled line resulting from the sum of the relative plate motion and the motion of the hotspot (indicated by the dark hotspot track and the arrows at the spreading ridge.)

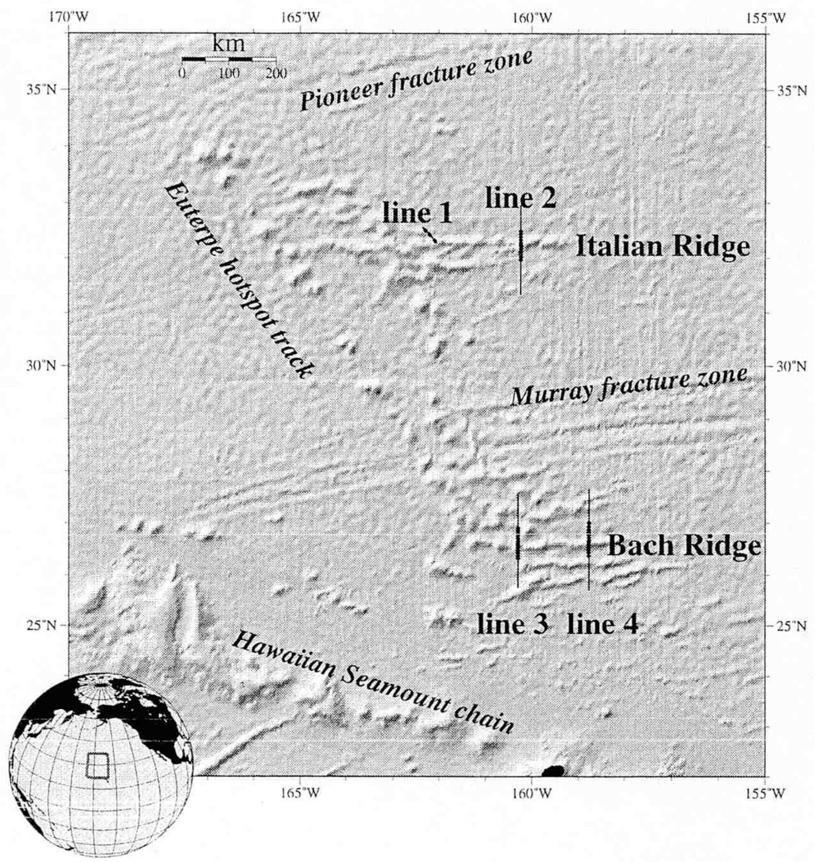
170°W
165°W
160°W
155°W
km
0 100 200
35°N
30°N
25°N
Pioneer fracture zone
Euterpe hotspot track
line 1
line 2
Italian Ridge
Murray fracture zone
Bach Ridge
line 3
line 4
Hawaiian Seamount chain

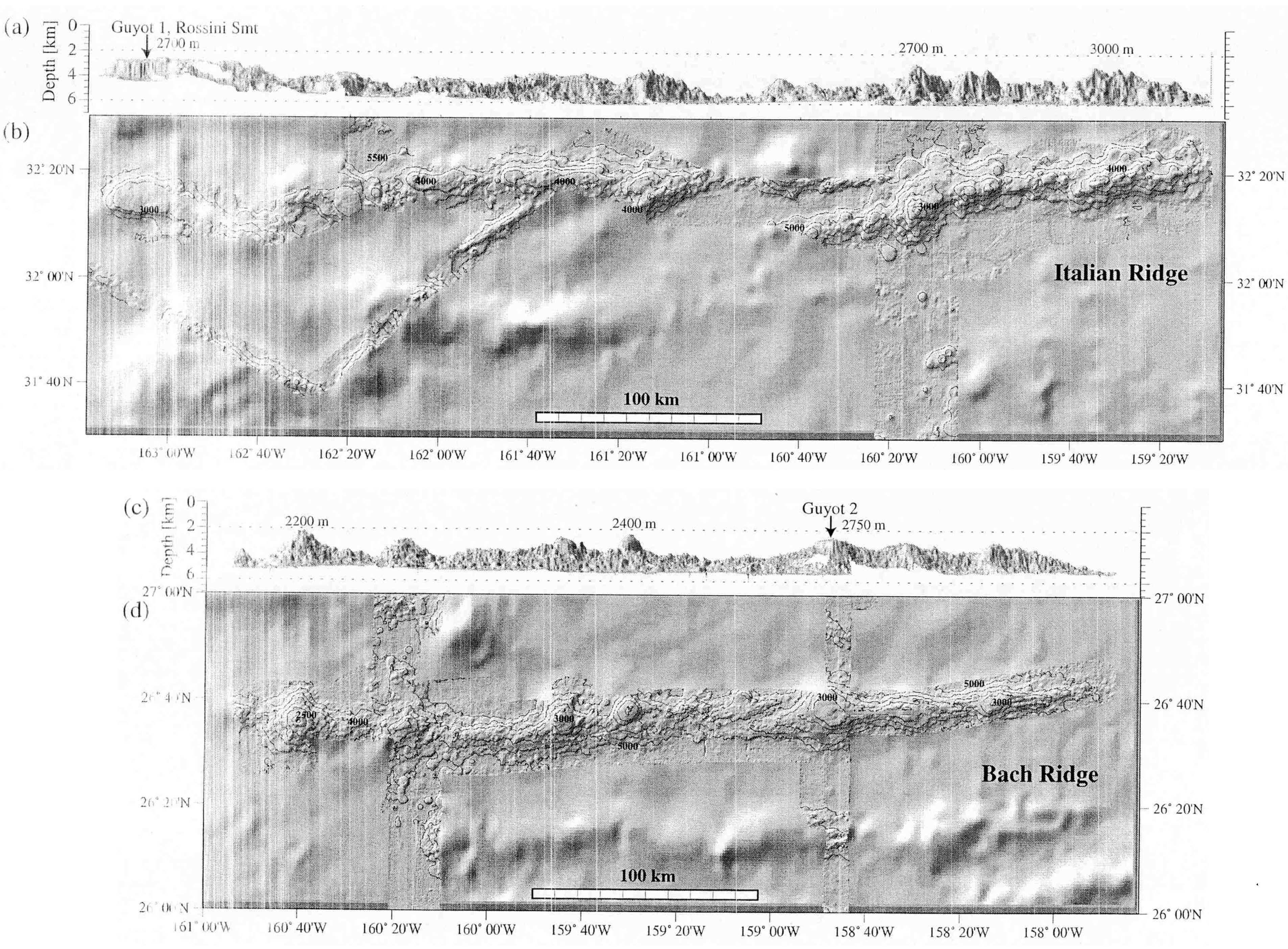

(a)
Depth [km]
Guyot 1, Rossini Smt
2700 m
2700 m
3000 m
(b)
Italian Ridge
100 km
32° 20'N
32° 00'N
31° 40'N
163° 00'W
162° 40'W
162° 20'W
162° 00'W
161° 40'W
161° 20'W
161° 00'W
160° 40'W
160° 20'W
160° 00'W
159° 40'W
159° 20'W
(c)
Depth [km]
2200 m
2400 m
Guyot 2
2750 m
(d)
Bach Ridge
100 km
27° 00'N
26° 40'N
26° 20'N
26° 00'N
161° 00'W
160° 40'W
160° 20'W
160° 00'W
159° 40'W
159° 20'W
159° 00'W
158° 40'W
158° 20'W
158° 00'W

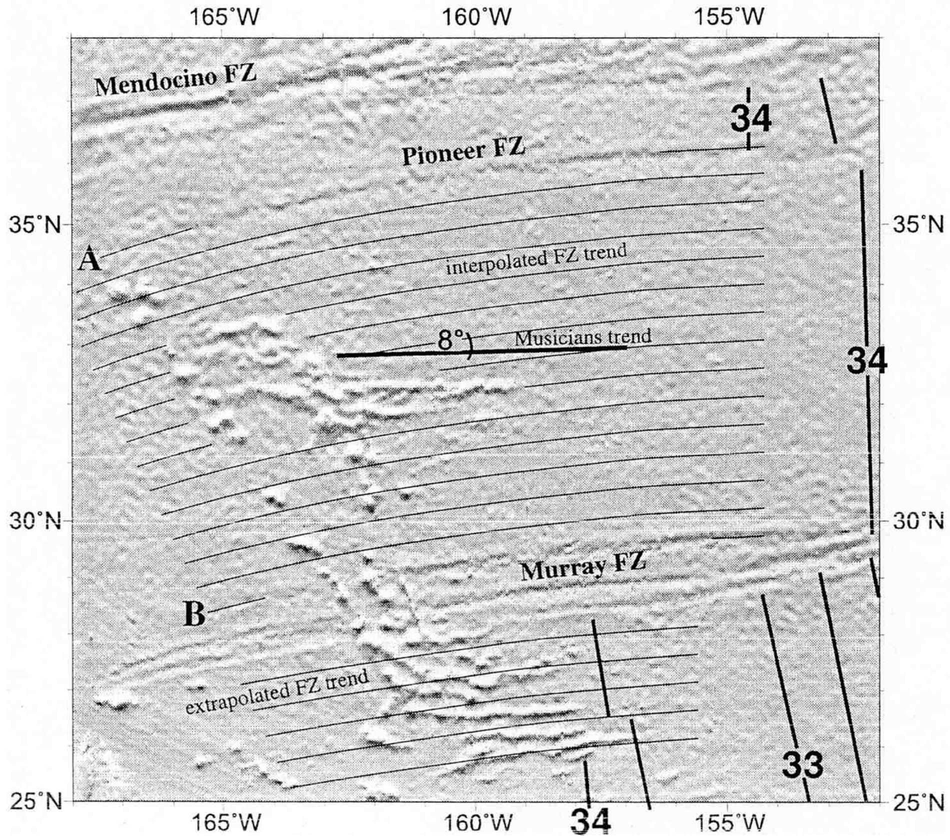
165°W
160°W
155°W
Mendocino FZ
34
Pioneer FZ
35°N
A
interpolated FZ trend
8°
Musicians trend
34
30°N
Murray FZ
B
extrapolated FZ trend
33
25°N
34

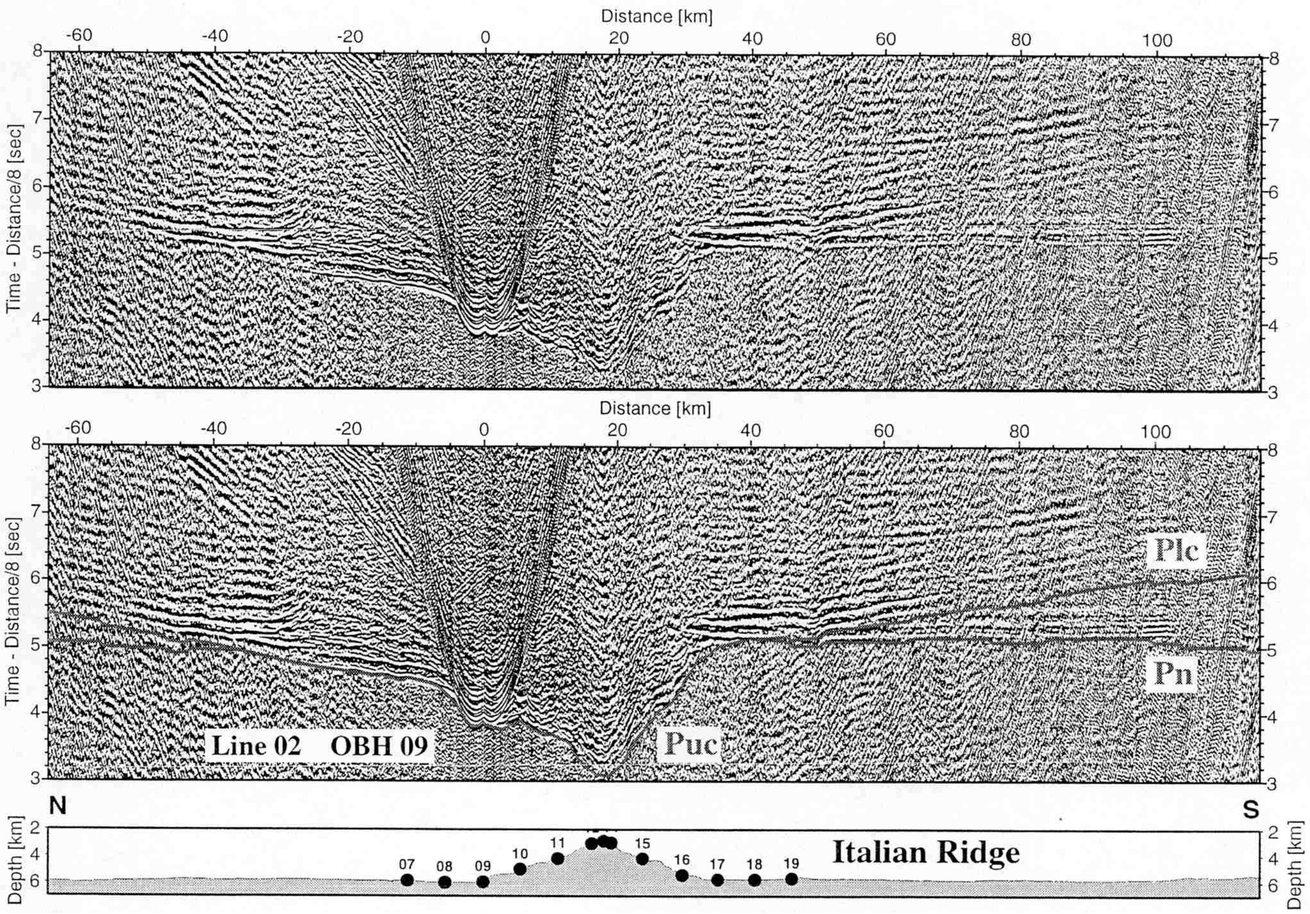
Distance [km]
Time - Distance/8 [sec]
Plc
Pn
Puc
Line 02 OBH 09
N
S
Depth [km]
Italian Ridge
07 08 09 10 11 15 16 17 18 19

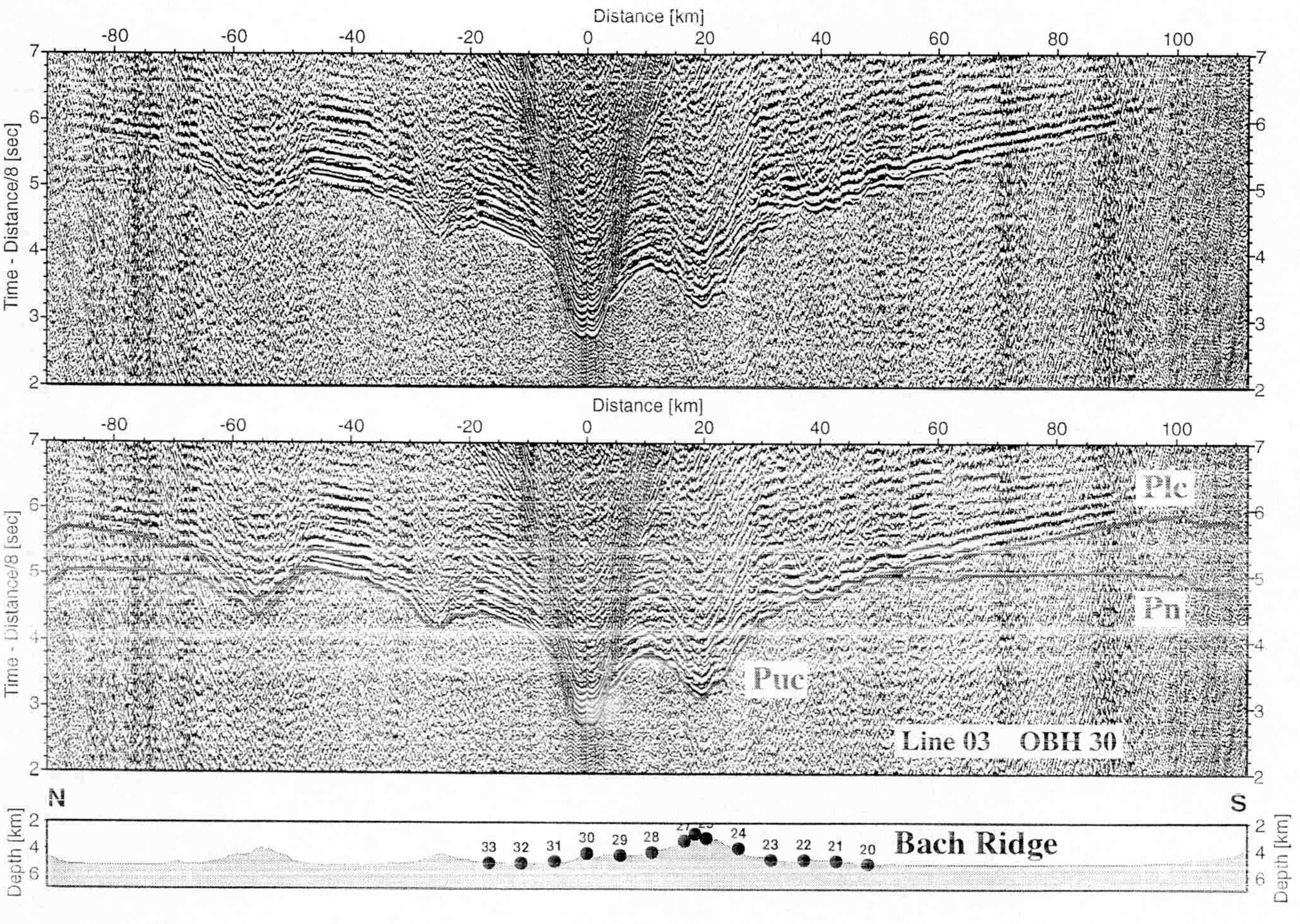
Distance [km]
Time - Distance/8 [sec]
Plc
Pn
Puc
Line 03 OBH 30
N
S
Depth [km]
Bach Ridge
33 32 31 30 29 28 27 24 23 22 21 20

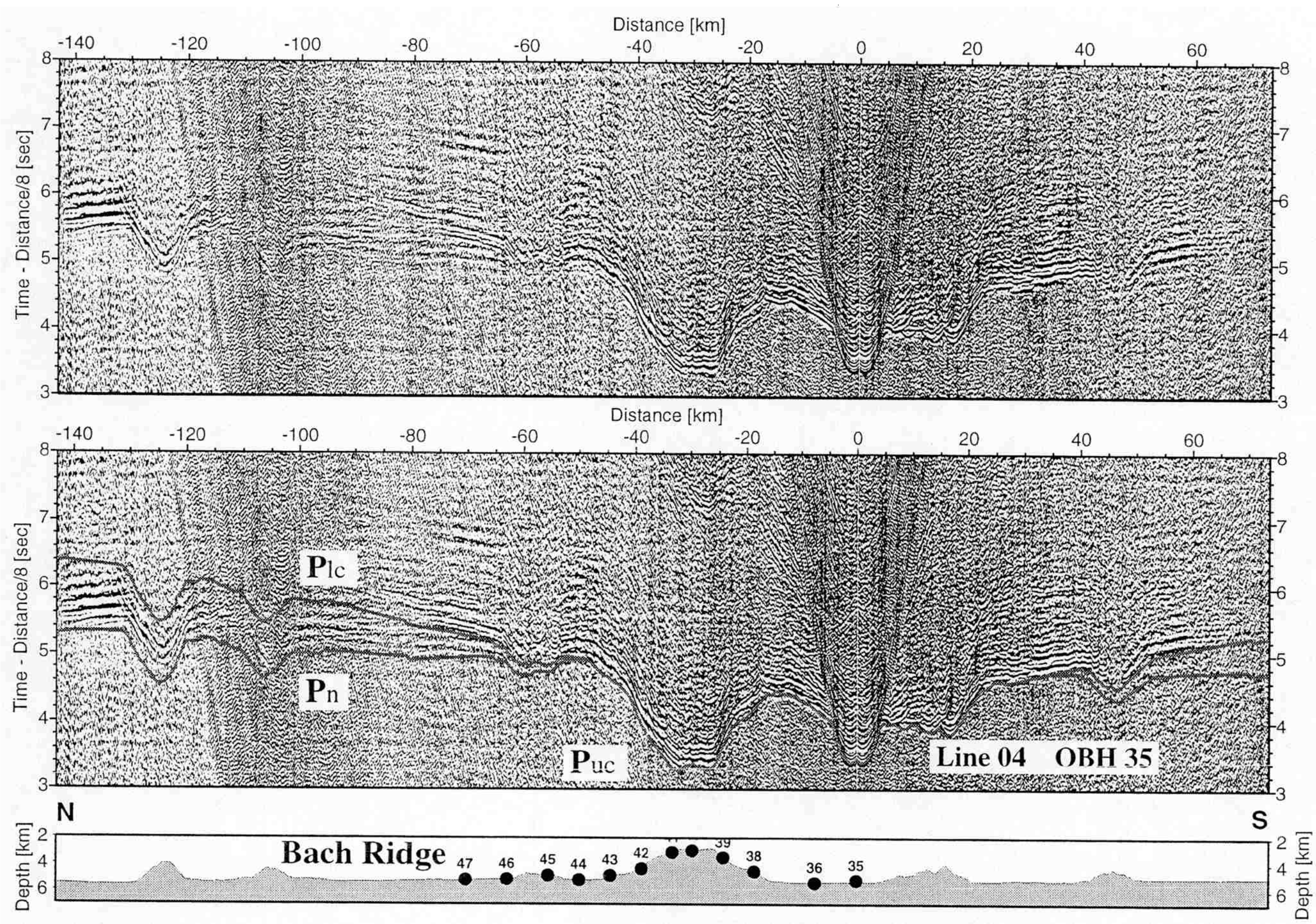
Distance [km]
Time - Distance/8 [sec]
Plc
Pn
Puc
Line 04 OBH 35
N
S
Bach Ridge
Depth [km]
47
46
45
44
43
42
39
38
36
35

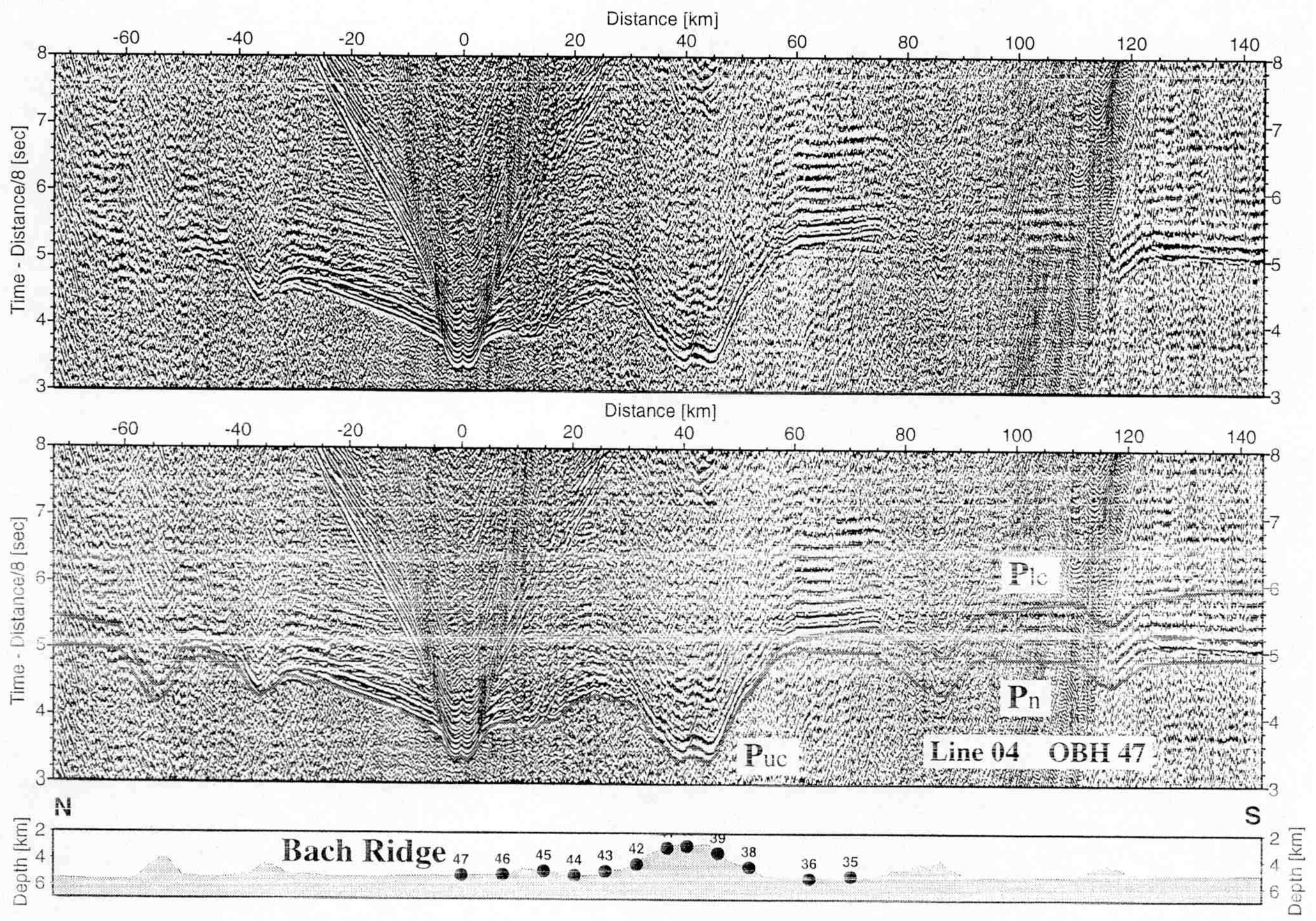
Distance [km]
Time - Distance/8 [sec]
Plc
Pn
Puc
Line 04 OBH 47
N
S
Bach Ridge
Depth [km]
47
46
45
44
43
42
39
38
36
35

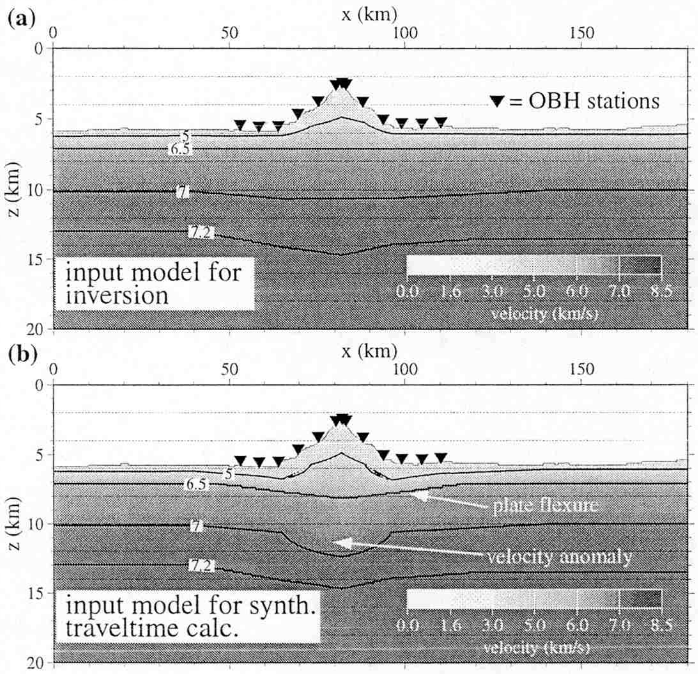

(a)
x (km)
0
50
100
150
0
5
10
15
20
z (km)
▼ = OBH stations
5
6.5
7
7.2
input model for
inversion
0.0 1.6 3.0 5.0 6.0 7.0 8.5
velocity (km/s)
(b)
x (km)
0
50
100
150
0
5
10
15
20
z (km)
5
6.5
7
7.2
plate flexure
velocity anomaly
input model for synth.
traveltime calc.
0.0 1.6 3.0 5.0 6.0 7.0 8.5
velocity (km/s)

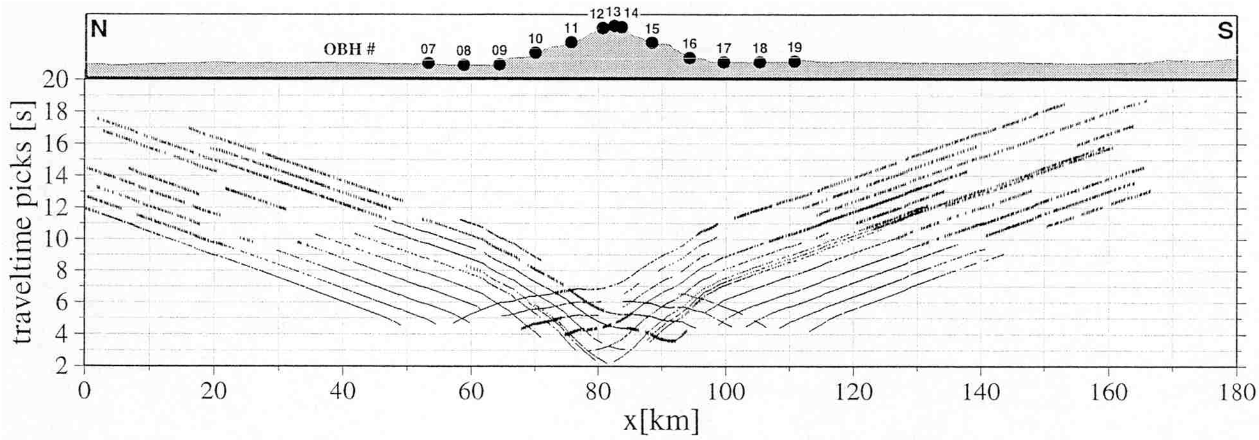
N
S
OBH #
07
08
09
10
11
12
13
14
15
16
17
18
19
traveltime picks [s]
x[km]
20
18
16
14
12
10
8
6
4
2
0
20
40
60
80
100
120
140
160
180

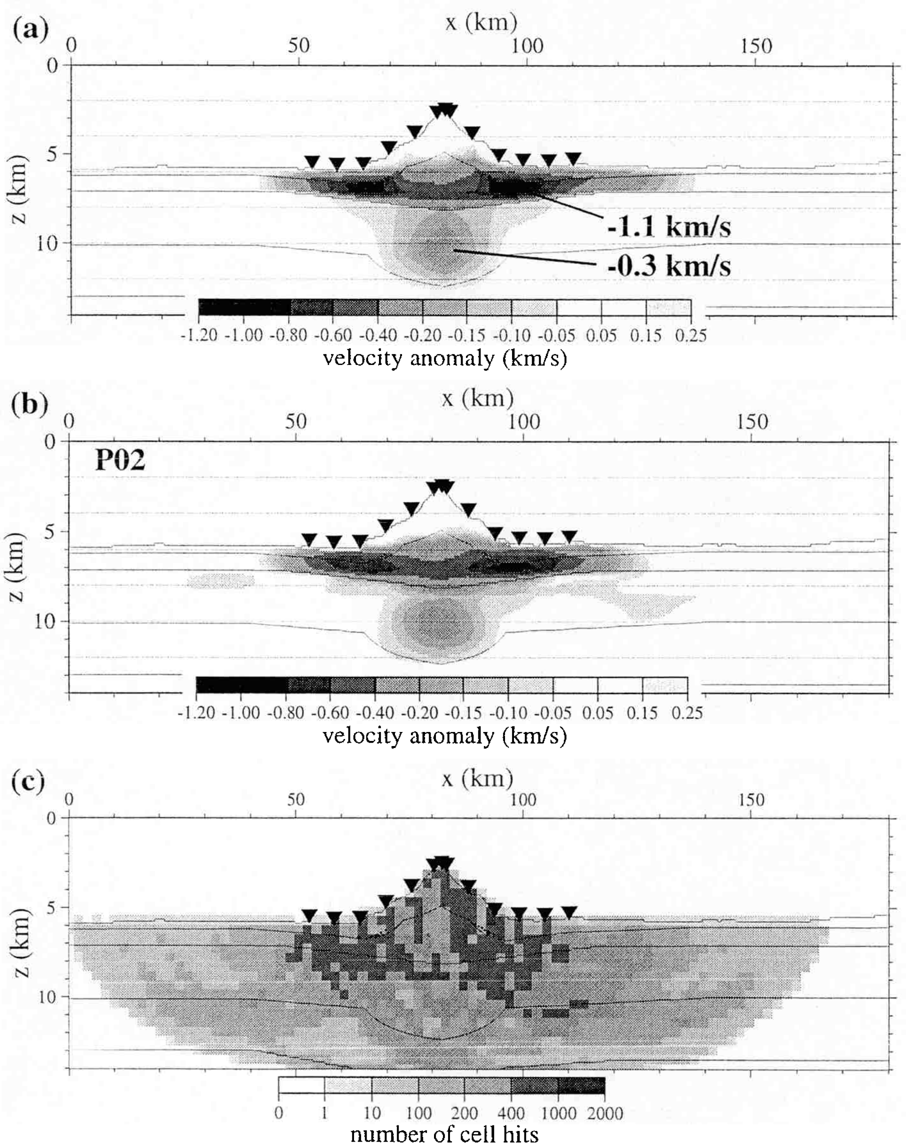
(a)
x (km)
0
50
100
150
0
5
10
z (km)
-1.1 km/s
-0.3 km/s
-1.20 -1.00 -0.80 -0.60 -0.40 -0.20 -0.15 -0.10 -0.05 0.05 0.15 0.25
velocity anomaly (km/s)
(b)
x (km)
P02
-1.20 -1.00 -0.80 -0.60 -0.40 -0.20 -0.15 -0.10 -0.05 0.05 0.15 0.25
velocity anomaly (km/s)
(c)
x (km)
0 1 10 100 200 400 1000 2000
number of cell hits

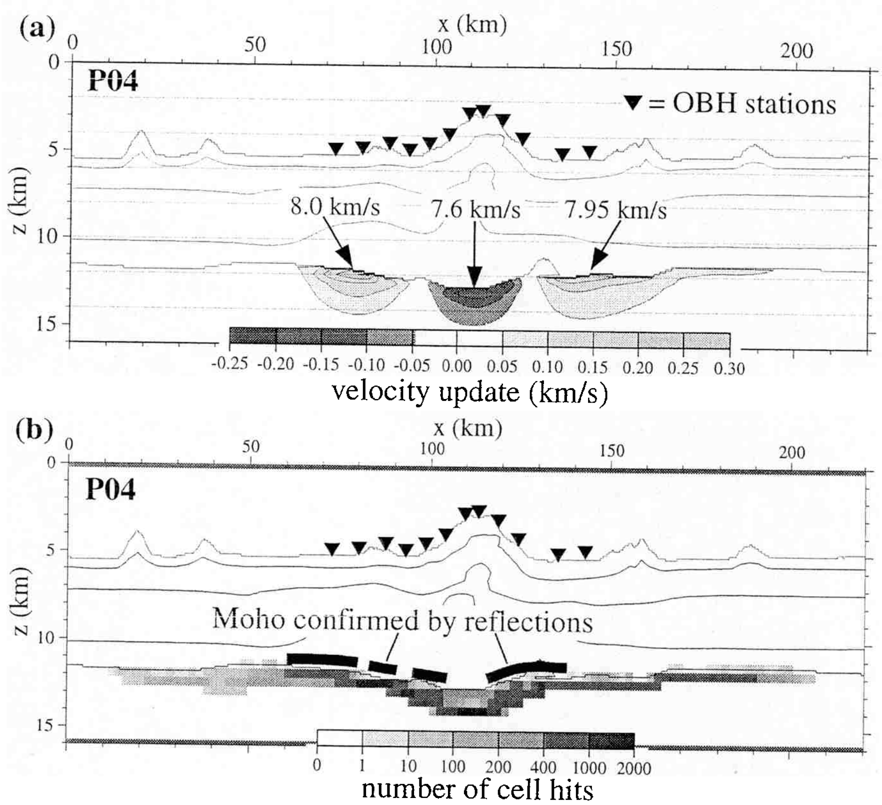
(a)
x (km)
P04
▼ = OBH stations
z (km)
8.0 km/s
7.6 km/s
7.95 km/s
velocity update (km/s)
(b)
x (km)
P04
z (km)
Moho confirmed by reflections
number of cell hits

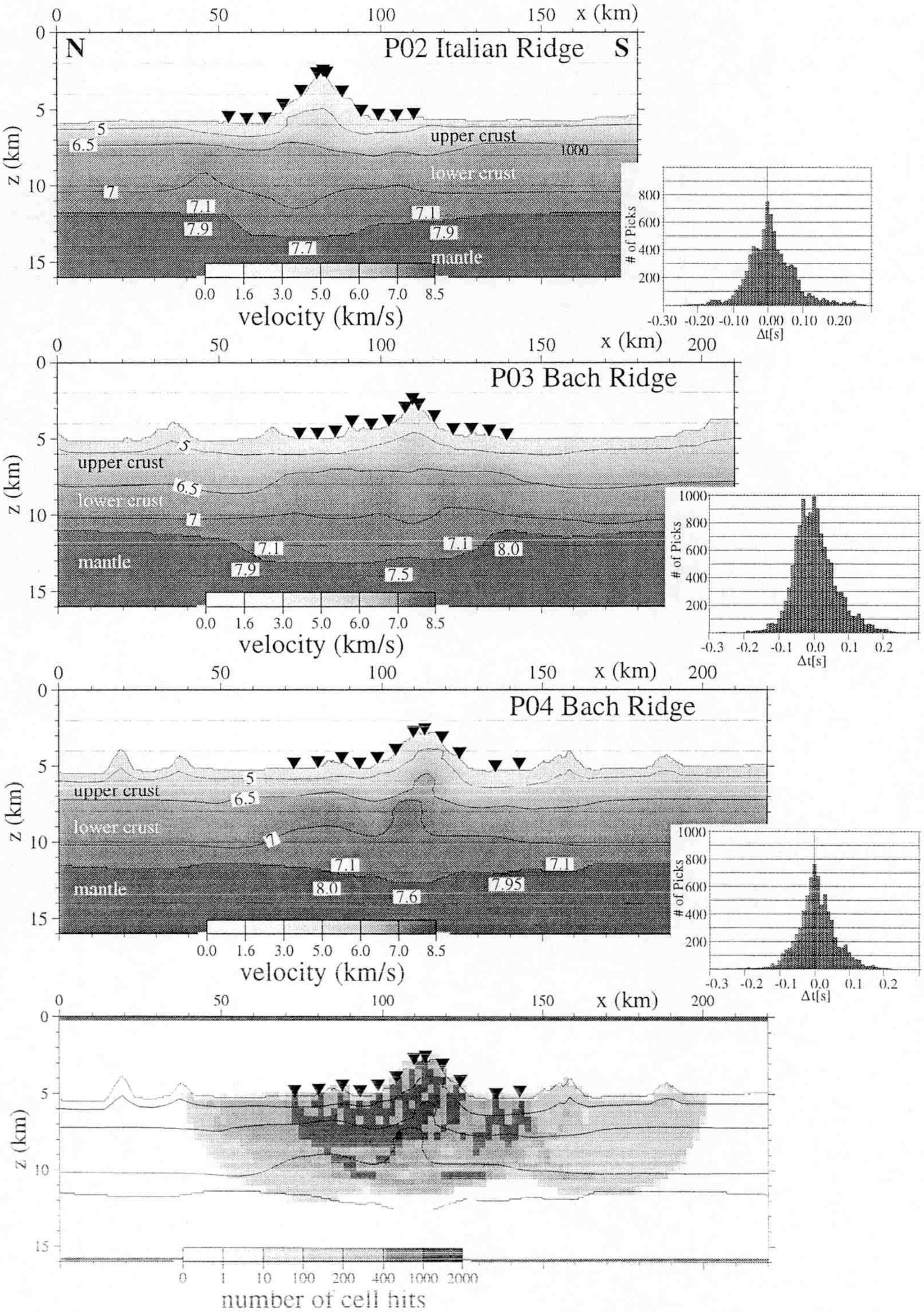
P02 Italian Ridge
N
S
x (km)
z (km)
upper crust
lower crust
mantle
1000
7.1
7.9
7.7
velocity (km/s)
0.0 1.6 3.0 5.0 6.0 7.0 8.5
# of Picks
Δt[s]
P03 Bach Ridge
upper crust
lower crust
mantle
7.1
7.9
7.5
8.0
velocity (km/s)
P04 Bach Ridge
upper crust
lower crust
mantle
7.1
8.0
7.6
7.95
velocity (km/s)
number of cell hits
0 1 10 100 200 400 1000 2000

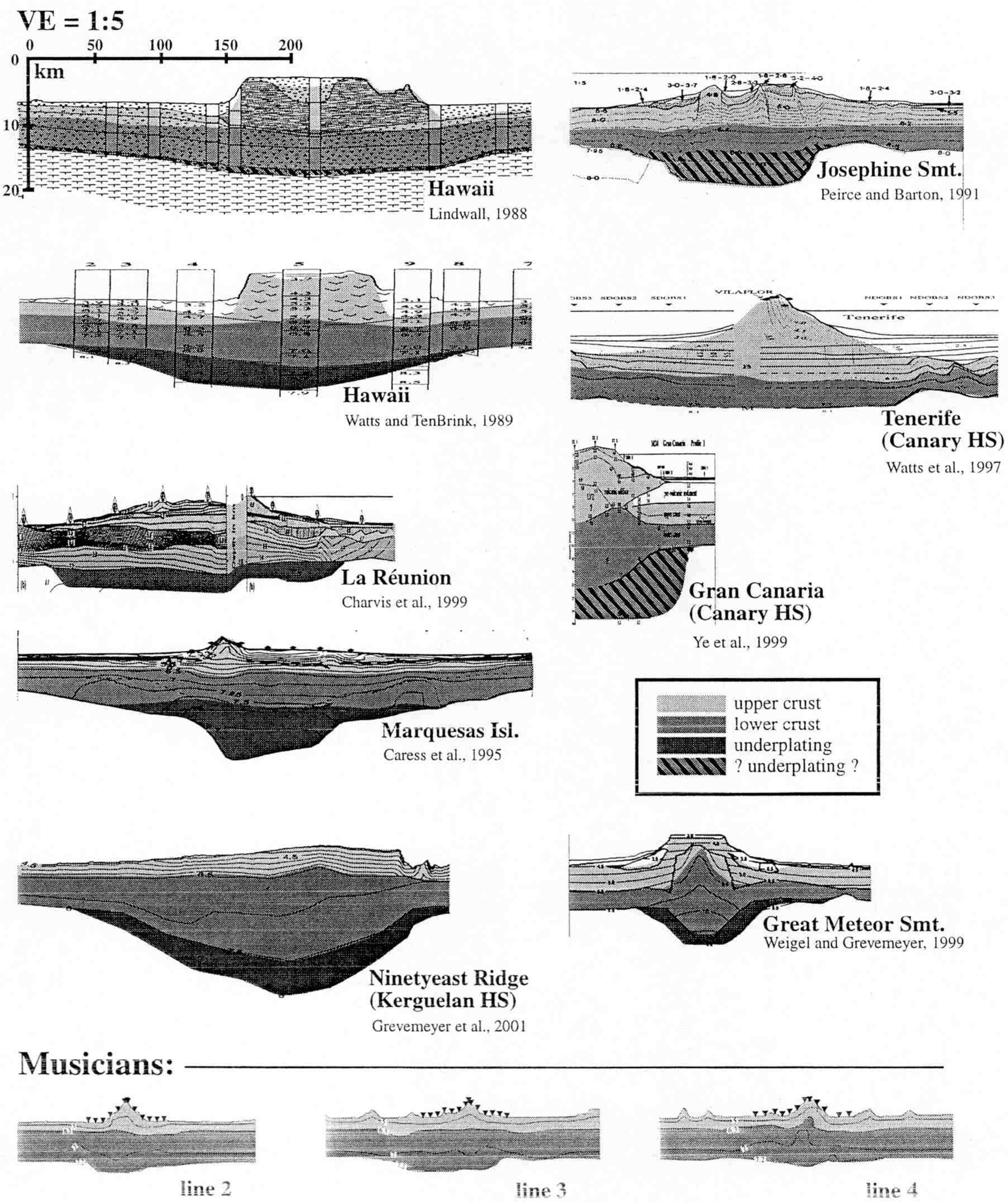
VE = 1:5
0 50 100 150 200
km
0
10
20
Hawaii
Lindwall, 1988
Josephine Smt.
Peirce and Barton, 1991
Hawaii
Watts and TenBrink, 1989
Tenerife
(Canary HS)
Watts et al., 1997
La Réunion
Charvis et al., 1999
Gran Canaria
(Canary HS)
Ye et al., 1999
Marquesas Isl.
Caress et al., 1995
upper crust
lower crust
underplating
? underplating ?
Ninetyeast Ridge
(Kerguelan HS)
Grevemeyer et al., 2001
Great Meteor Smt.
Weigel and Grevemeyer, 1999
Musicians:
line 2
line 3
line 4

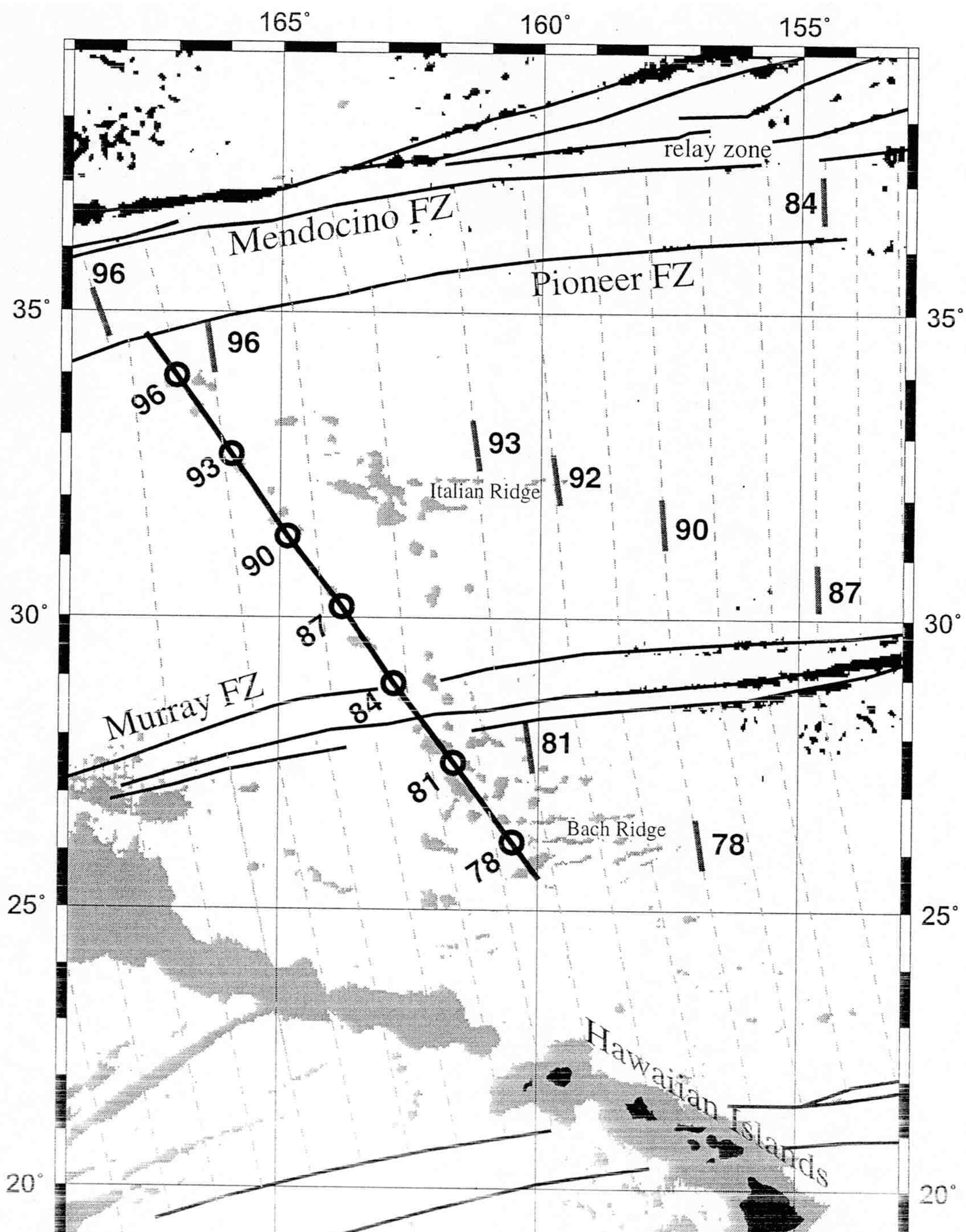

165°
160°
155°
relay zone
84
Mendocino FZ
96
Pioneer FZ
35°
96
96
93
93
92
Italian Ridge
90
90
87
87
30°
Murray FZ
84
81
81
Bach Ridge
78
78
25°
Hawaiian Islands
20°

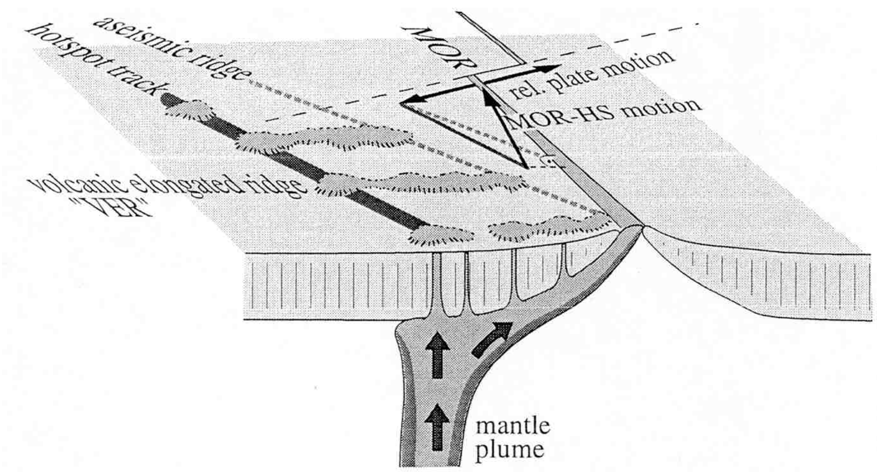
aseismic ridge
hotspot track
MOR
rel. plate motion
MOR-HS motion
volcanic elongated ridge
"VER"
mantle
plume

01. 8. 02